Geological Society of America
Special Paper 388
2005

Primary magmas at mid-ocean ridges, "hotspots," and other intraplate settings: Constraints on mantle potential temperature

David H. Green*
Research School of Earth Sciences, Australian National University, Canberra 0200, ACT, Australia
Trevor J. Falloon*
Research School of Earth Sciences, Australian National University, Canberra 0200, ACT, Australia,
and *School of Earth Sciences, University of Tasmania, Hobart 7001, Tasmania*

ABSTRACT

Intraplate, "hotspot," and mid-ocean ridge basalts (MORB) are characteristic of the modern Earth, and within the plate tectonics interpretation of the Earth's behavior become the basis for a petrological model of the lithosphere and asthenosphere. This model is based on experimental studies of various primitive magmas and of peridotite + (C-H-O), including melting and phase relationships under variable oxygen fugacities (fO_2). The deep mantle plume hypothesis requires a large potential temperature difference (ΔT_p 200–250 °C) between the upwelling plume and normal ambient mantle as sampled by mid-ocean ridge upwelling and by nonplume intraplate basalts. This core tenet of the deep mantle plume hypothesis is testable by comparison of primitive hotspot magmas with intraplate magmas and particularly with primitive MORB.

We have examined picrites and olivine phenocryst compositions from Hawaiian volcanoes and a large new dataset of glass compositions from the Hawaiian Scientific Drilling Project, sampling deep into the main cone-building phase of Mauna Kea volcano. By incremental addition of olivine (reversing the crystallization of magmas saturated only in olivine + Cr-Al spinel) we infer the parental or primitive picrite magma compositions for distinctive compositional suites and individual volcanoes. We then calculate liquidus temperatures (1 atm) and infer conditions of melt separation from residual lherzolite (olivine + orthopyroxene + clinopyroxene ± spinel) or harzburgite (olivine + orthopyroxene + Cr spinel). The Hawaiian tholeiitic picrites of the main shield-building phase consistently indicate harzburgite residue and pressures of magma segregation around 1.5–2 GPa.

The petrological database of glass compositions from mid-ocean ridge settings contains more than 190 analyses of glass with more than 9.5% MgO. These quenched liquids were saturated in olivine (mole $MgO/(MgO + FeO_t)$ or Mg # = 86–89) and Al-Cr spinel. Olivine addition calculations are used to estimate parental liquid compositions with liquidus olivine Mg # = 90.5–91.5. Further constraint is provided by the requirement that parental liquids lie on ol + opx ± cpx + spinel saturation surfaces for a lherzolitic or harzburgitic residue. We infer primitive or parental MOR magmas to be picrites with 13%–16% MgO, segregating from lherzolite to harzburgite residue for the most part at ~2 GPa but in some cases at pressures as low as 1 GPa. Our analysis

*E-mails: david.h.green@anu.edu.au; trevor.falloon@utas.edu.au.

Green, D.H., and Falloon, T.J., 2005, Primary magmas at mid-ocean ridges, "hotspots," and other intraplate settings: Constraints on mantle potential temperature, *in* Foulger, G.R., Natland, J.H., Presnall, D.C., and Anderson, D.L., eds., Plates, plumes, and paradigms: Geological Society of America Special Paper 388, p. 217–247.

of the compositions and liquidus temperatures of parental magmas at a hotspot (Hawaii) and at mid-ocean ridge settings finds that picritic magmas with >13% MgO are characteristic of both settings. Liquidus temperatures have the same range, to a maximum of 1380–1390 °C if volatile-free, but up to 1335 °C (Hawaii) and ~1355 °C (mid-ocean ridges) if volatiles (C-H-O) are included.

The maximum temperatures of primitive magmas and the inferences from the systematics of peridotite partial melting are used to estimate mantle potential temperatures of ~1430 °C at mid-ocean ridges and up to 1400 °C beneath Hawaiian volcanoes. The principal differences between hotspot and MOR primitive magmas are compositional and not thermal. The hotspot source has geochemical signatures that suggest melting, depletion, and refertilization processes in subduction settings, as well as enrichment processes due to migration of incipient melt (carbonatite to olivine nephelinite) in the asthenosphere. The melting and primary differentiation of the Earth's mantle observed at divergent plate boundaries and in intraplate settings, including hotspots, is a consequence of the plate tectonics cycle's acting on the modern Earth with T_p 1430 °C. Plate tectonics introduces chemical inhomogeneity, including redox contrasts, into the Earth's upper mantle, and chemical heterogeneity within the asthenosphere and upper mantle (i.e., below the lithospheric plates) at T_p 1430 °C, together with global degassing of (C-H-O) fluids, is responsible for the diverse intraplate, hotspot, and MOR magmas.

Keywords: primary magmas, mantle temperature, mantle volatiles

INTRODUCTION AND BACKGROUND

The term "hot spot" was first used in global tectonics by Carey (1958) in discussions of the volcanic island chains of the Atlantic, for which he coined the term "nematath." Carey (1958, p. 195) said that nemataths "join points which were originally closer, and mark the path of separation movement, . . . where the rifting line crosses a zone of higher isotherms (i.e., a volcanic zone)," and also (p. 227) wrote of the "suggested 'hot spot' origin of nemataths" in discussion of the Walvis ridge in the Atlantic. Wilson (1963) emphasized the sequential eruption of Hawaiian volcanoes, younging to the southeast, and similarly explained this by lithosphere migration across a stationary "hot spot" in the mantle. Morgan (1971) attributed a mechanism and cause for the thermal anomaly by proposing the existence of narrow thermally buoyant plumes arising in the deep mantle. Lithospheric plates, and divergent boundaries (mid-ocean rifts) of plates, are interpreted as shallow (≤250–300 km) phenomena that are observed to migrate with respect to a relatively fixed framework of deep mantle plumes representing long-lived convective features of the deep mantle, possibly sourced from a core-mantle thermal boundary layer (e.g., Davies 1998). With strong observational support and theoretical support from modeling of mantle convection, the "mantle plume" hypothesis is widely used in the geological literature and has become more complex, variable, and site-specific in its detail.

The purpose of this paper is to summarize the melting characteristics of the Earth's mantle and examine the primitive or parental magmas of typical mid-ocean ridge settings and those of the Hawaiian "hotspot" (as representative of "plume" volcanism) for information that they may reveal on the temperatures and compositions of their mantle sources. This exercise is a significant investigation of the "mantle plume" hypothesis, as a central tenet of this hypothesis is that temperature-induced buoyancy is required, with a prediction of a large temperature contrast of ≥200 °C between a rising mantle plume in the lower or upper mantle and normal ambient mantle. Mid-ocean ridge basalts (MORB) are interpreted as products of upwelling of normal mantle from asthenopheric depth, with the detail of upwelling varying with rates of ridge migration and spreading.

The earliest work on dredged ocean floor basalts (Engel et al., 1965) identified petrographic and major-element differences between magmas of this newly sampled volcanic setting and the well-studied Hawaiian hotspot or oceanic island chain. Thus while both magma types were identified as olivine tholeiite (i.e., olivine + hypersthene normative), the ocean floor basalts were termed "high-alumina" olivine tholeiites and petrographically showed olivine (+ spinel) and plagioclase phenocrysts whereas the Hawaiian olivine tholeiites characteristically showed olivine (+ spinel) + clinopyroxene phenocrysts, with plagioclase appearing later in the crystallization interval. These differences in major-element composition were then incorporated by Green and Ringwood (1967a), in the applications of their experimental high-pressure studies, into their proposals that primitive MORB (high-alumina olivine tholeiite) segregated from adiabatically upwelling lherzolitic ("pyrolite") mantle at ~1 GPa

whereas Hawaiian tholeiitic picrites to olivine-rich tholeiites segregated at higher pressures of ~1.5 GPa. Although specifically abandoned in later work (Green et al., 1979; Jaques and Green, 1980; Falloon and Green, 1988) this allocation of primitive MORB to ~1 GPa depth of magma segregation has remained in many discussions of MORB petrogenesis (e.g., McKenzie and Bickle, 1988; Presnall et al., 2002).

In later work the concept of distinctive chemical differences between "hotspot" and "MORB" primitive magmas was emphasized, particularly attributing relative enrichment in incompatible elements—large-ion lithophile elements (LILE) and light rare earth elements (LREE)—to hotspot sources and contrasting these with the chondritic to depleted ratios of incompatible elements in MORB. As sampling has increased, these geochemical signatures have become blurred with recognition that MORB may be enriched (E-MORB), normal (N-MORB), or depleted (D-MORB) in incompatible elements (particularly evident in the LREE) and that the MORB source regions show some isotopic heterogeneity. Similarly, Iceland, an on-ridge hotspot, has examples of both enriched (hotspot) and depleted (? MORB) incompatible-element ratios. However, increased knowledge has confirmed the greater heterogeneity (in minor- and trace-element contents and in isotopic composition) of hotspot magmas in contrast to more subdued variation among MORB magmas.

Although much emphasis has been placed on a twofold division of modern mantle-derived magmatism into MORB and ocean island basalts (OIB, equivalent to hotspot basalts), the OIB trace-element characteristics (LILE and LREE-enriched) and isotopic heterogeneity are also apparent in within-plate basaltic volcanism related to rifting or to other unidentified within-plate causes. Typically such volcanic centers are small in volume, and magma types range from extremely silica-undersaturated (carbonatites, olivine melilitites, kimberlites) to hypersthene-normative olivine tholeiites and quartz tholeiites. In spite of their limitations in volume, these magma types are very informative with respect to lithospheric composition and processes and to their conditions of genesis because they commonly contain xenoliths and xenocrysts preserving high-pressure mineralogy. These intraplate magmas provide lithosphere samples (dominantly but not only peridotite xenoliths) and identify themselves as liquids formed within the upper mantle (i.e., at depths at least as great as the depth from which xenoliths were entrained). They provide evidence on the nature of and the processes within the intraplate lithosphere and asthenosphere. Such high-pressure xenolith-bearing magmas occur within both oceanic and continental intraplate settings, and because intraplate settings dominate the Earth's surface in an areal sense, the information they reveal is of primary importance in interpreting the nature of Earth's lithosphere and asthenosphere. If we can correctly interpret the intraplate characteristics of the Earth, the singular perturbations of the intraplate settings marked by hotspots and the processes at the plate margins (convergent, conservative-transform, and divergent) can probably be understood better.

Intraplate volcanism produces an extraordinary variety of magmas including minor carbonatitic and sulphidic melts and more voluminous silicate magmas. It is also able to generate fluids, dominantly fluids rich in CO_2, CH_4, or H_2O. Petrological research attempts to understand the causes of this diversity among the products of mantle melting. There is another approach to magma genesis that emphasizes geophysical constraints on mantle characteristics, including melting and magmatism. The latter approach at least begins with a single mantle composition and solidus and seeks clear definition of parameters such as melt fraction as functions of pressure and temperature, as well as porosity-permeability relations to constrain melt extraction and porous melt flow. As a first step, Earth models assume chemical compositional homogeneity and operate with variable pressure, temperature, and phase stability. The different approaches must be reconciled, and in this paper we emphasize the extraordinary complexity of melting relations in a lherzolite composition in the presence of carbon, hydrogen, and variable oxygen activities. We follow this by examining primitive magmas themselves for evidence of their temperatures, and thus the temperatures of their source regions. We then address the further complexity introduced to both petrogenesis and geodynamic models if compositional heterogeneity is considered. *The focus is on the behavior of the modern Earth so that the plate tectonics framework of coherent lithospheric plates, the formation and later subduction of oceanic crust and lithosphere, etc., is accepted. Thus it is accepted that the peridotitic mantle differentiates at divergent plate boundaries to yield basaltic crust and is chemically modified and rendered heterogeneous by subduction processes.*

In addressing the related issues of the mantle compositions and genesis of basaltic magmas, we take the position that primitive mantle-derived magmas have compositions determined by equilibrium partial melting of a peridotitic source and that they retain the compositional signature of a "depth of magma segregation." This concept asserts that there is a pressure-temperature (*P-T*) condition at which a primitive magma was in chemical equilibrium with residual olivine, orthopyroxene and other phases (clinopyroxene, spinel, plagioclase, garnet) appropriate to the degree and depth of partial melting. A "source composition" may be calculated from magmas and residual phase compositions and their relative proportions. The concept does not define or require a specific process of assembling or generating the source composition at the depth of magma segregation. The concept is obviously able to be investigated by experimental high-pressure, high-temperature methods and is commonly referred to as a "batch melting" approach to magma genesis.

This approach is appropriate if melt extraction from partial melting of lherzolite is governed by a threshold porosity of >1%–2% melt, at which melt permeability rapidly increases (Faul, 2001), particularly if mantle upwelling is dynamic and has the character of a "plume," "diapir," or "thermal"—i.e., a 3D buoyant upwelling bounded by significant temperature gradients against enclosing mantle. An alternative model of melting, presented for continuous oceanic crust and lithosphere formation

at spreading centers, is based on passive upwelling and very low melt retention, so melting approaches polybaric fractional melting and there is "instantaneous" melt extraction and melt pooling (McKenzie and Bickle, 1988). MORB are interpreted as mixtures of near-solidus melt increments derived from the *P-T* and compositional variance within the modeled melt volume and focused melt flow. In this approach, although individual melt increments have compositions determined by the *P-T* and bulk composition (fertile at first entry into the partial melting regime to very refractory at the apex of the melting volume immediately beneath the ridge axis), the aggregated melt (primitive MORB) does not represent equilibrium between melt and residual phases at the depth of pooling or aggregation. Green and Falloon (1998) give a more detailed discussion of reasons for preferring the "diapir" or 3D, buoyant or dynamic, upwelling model of magma genesis.

INTRAPLATE MAGMAS AND LITHOSPHERE AND ASTHENOSPHERE DEFINITION

Intraplate basaltic volcanism includes, at one extreme, the voluminous continental flood basalt provinces and possibly similar phenomena in an ocean basin setting, i.e., large igneous provinces or ocean plateaus such as the Ontong-Java plateau. At the other extreme are kimberlites, carbonatites, and silicate magmas such as olivine leucitite or lamproite and olivine melilitite, which are extremely small-volume melts that are commonly erupted along crustal fractures and associated with incipient rifting and within-plate deformation. Between these extremes are common rift-related basaltic provinces in which olivine nephelinites, olivine-rich basanites, alkali olivine basalts, and olivine tholeiites (and their fractionation products) are represented, with the relative volumes increasing in this order. In seeking to understand this wide spectrum of magmas in terms of mantle processes, a first step is to note that if the Earth's upper mantle is peridotitic with olivine of mole $MgO/(MgO + FeO_t)$ or Mg # = 90, basaltic liquids directly segregating from such mantle have Mg # ~ 75. If we apply this criterion to the spectrum of intraplate magmas noted earlier, continental flood basalt provinces are dominated by fractionated magmas, typically quartz tholeiites of Mg # < 65. Potential primary magmas are rare tholeiitic picrites with Mg # > 70 and most magnesian olivine phenocrysts of Mg # ≥ 89.

If the primary magma test is applied to those intraplate volcanoes that also contain high-pressure, mantle-derived xenoliths, many, ranging from kimberlites through olivine leucitites and from olivine melilitites to alkali olivine basalts, have the required primary characteristic of Mg # > 70. (There is a degree of uncertainty in estimating olivine–liquid Mg/Fe partitioning because of using Fe_{total} and not distinguishing Fe^{2+} and Fe^{3+}.) However, there are also mantle-derived magmas containing high-pressure xenoliths that have low Mg # and that evolved as derivative magmas formed by cooling, crystallization, and wall-rock reaction within the upper mantle. These evolved magmas of upper mantle derivation include slightly hypersthene-normative hawaiite, mugearite, nepheline mugearite, and even phonolite (Green and Hibberson, 1970; Price and Green, 1972; Green et al., 1974). The complementary component to these mantle-fractionated liquids include mafic xenocrysts and xenoliths of dunite, pyroxenite, spinel pyroxenite, hornblende pyroxenite, and garnet pyroxenite with Mg # of phases <90. These types of xenolith commonly show initial high-temperature mineralogy partially equilibrating to lower temperatures while remaining at high pressure. Studies of mantle xenoliths and their host magmas may give detailed insights into the evolution of lithosphere and asthenosphere in particular localities (e.g., Worner and Zipfel, 1996). They demonstrate that the lithosphere becomes heterogeneous in composition and that many magmas of both primitive and evolved character are formed within the upper mantle rather than by processes of near-fractional polybaric melting and melt pooling at shallow depths.

A second type of xenolith found in kimberlitic or related pipes and diatremes in continental settings is dominated by eclogite or garnet pyroxenite and may include minor phases of rutile, sanidine, kyanite, quartz, coesite, graphite, biotite, and diamond. These rock types are normally relatively Fe-rich (Mg # < 80) and are commonly explained as relict subducted oceanic crust (e.g., Schulze et al., 2003).

This brief summary of mantle xenoliths emphasizes the dominance of aluminous spinel-bearing lherzolites (olivine > orthopyroxene > clinopyroxene > spinel) with rare plagioclase + spinel lherzolites and garnet + spinel lherzolites. With decreasing clinopyroxene and increasing Cr # [100 Cr/(CR + Al)] in spinel, the lherzolites are transitional to harzburgite with little or no clinopyroxene. Pargasitic amphibole (or its decompression melting products of olivine + clinopyroxene ± plagioclase + spinel + glass) is a common minor phase, and phlogopitic mica is uncommon and sometimes located in veins and micro-shear zones. Modal metasomatism, interpreted as penetration and reaction of basaltic magma, is illustrated by mineral assemblages with abundant hornblende and minor apatite (O'Reilly and Griffin, 1988), and a further distinctive metasomatism (cryptic metasomatism), shown by increasing clinopyroxene relative to orthopyroxene, minor apatite, and CO_2-rich fluid inclusions, is attributed to decarbonation reactions of sodic-dolomitic carbonatite melt (Green and Wallace, 1988; Yaxley et al., 1991; Yaxley and Green, 1996; Yaxley et al., 1998).

The observations from mantle xenoliths and their host magmas may be summarized as follows:

1. The intraplate lithosphere is dominantly lherzolite with olivine of Mg # = 89–91 but variable from "fertile" at 3%–4% CaO, Al_2O_3 to refractory harzburgite or dunite with <1% CaO, Al_2O_3. In addition to compositional heterogeneity of this nature, greater heterogeneity is shown by small bodies of pyroxenite, spinel or garnet pyroxenite, and amphibolite of lower Mg #. These lithologies are attributed to precipitation and wall-rock reaction in magma chambers

and channels within the intraplate lithosphere. In continental lithosphere, as sampled by kimberlitic and related magmas, there may also be eclogitic materials inferred to be relict subducted oceanic crust.

2. The melting regime for mantle-derived basaltic magmas in intraplate settings (kimberlites to tholeiitic picrites) requires the presence of carbon and hydrogen (dissolved $CO_3^=$ and OH^-) in the melt phase.
3. Volume and compositional relationships among intraplate magmas argue that tholeiitic picrites represent large melt fractions of the mantle source, with kimberlites, olivine leucitites, and olivine melilitites representing very small melt fractions and (on the basis of their xenolith suites) magma segregation and transport from deeper levels.

EXPERIMENTAL STUDIES OF PERIDOTITE + (C-H-O)

The observations described earlier lead directly to the experimental study of the lherzolite + (C-H-O) system as a basis for understanding the nature of the intraplate lithosphere and asthenosphere and for understanding the genesis of intraplate basalts. The experimental study has proceeded on two parallel paths. The "forward" approach is the direct study of melting behavior of model lherzolitic mantle compositions with the aim of full documentation of residual phase and equilibrium melt compositions and the use of modal estimates and mass balance tests to determine the melt fraction and proportions of residual phases. In the forward approach the selection of a model mantle composition is important, and, because of their very large effect on melting behavior, the roles of small amounts of carbon and hydrogen, along with a range of oxidation states, are essential factors. The forward approach is experimentally very difficult for determination of melt composition because liquids commonly do not quench to glass or are compositionally modified in the quenching process.

The second approach, sometimes called the "inverse" approach, is to study the primary or primitive magmas themselves and use the experimental high-pressure, high-temperature techniques to determine the nature and composition of *liquidus phases* for a range of pressure, temperature, and dissolved C-H-O species. The rationale is that a primary magma segregating from residual peridotite is in equilibrium with residual phases of the peridotite at a particular *P-T* and dissolved volatile (C-H-O) component. Noting that all basaltic magmas show a contraction of the liquidus field for olivine with increasing pressure and an expansion of the liquidus fields for orthopyroxene or clinopyroxene with increasing pressure, the experimental approach is to seek, for pressure, temperature, and dissolved (C-H-O) conditions at which the potential primitive magma is saturated with olivine, orthopyroxene, and spinel, possibly together with clinopyroxene, and plagioclase, or garnet, or amphibole, or phlogopite (for magmas likely to be small melt fractions). As the ratio of melt to crystals is large for near-liquidus experiments, the likelihood that the melt will quench to glass without quench modification is enhanced. Techniques such as the "sandwich technique" (forcing a layer of basaltic liquid to react and reequilibrate with a layer of "source peridotite") and the "carbon aggregate" technique (using a porous layer of diamond or vitreous carbon spheres to extract the melt from residual peridotite) are used to avoid particular difficulties and can be evaluated for internal consistency of the data obtained.

Selection of Peridotite Compositions

The calculation of model compositions "Hawaiian pyrolite" and "mid-ocean ridge pyrolite" as source compositions for Hawaiian olivine tholeiite and mid-ocean ridge olivine tholeiite was reviewed by Green and Falloon (1998). For both compositions, liquid and residue were combined to give lherzolite compositions with Mg # = 89–90, 3%–3.5% CaO, and 3.5%–4.5% Al_2O_3, which are consistent with the most "fertile" of mantle xenoliths and high-pressure, high-temperature peridotite intrusions. A third natural lherzolite composition (Tinaquillo lherzolite) is very similar in MgO, FeO, CaO, SiO_2, and Al_2O_3 but is depleted in Na_2O, TiO_2 and very depleted in K_2O, P_2O_5 and other strongly incompatible elements. These three compositions represent a spectrum from incompatible-element-enriched mantle ("hotspot" or "enriched mantle") through normal upper mantle (N-MORB source or "fertile" mantle) to depleted mantle (Tinaquillo lherzolite, ? D-MORB source mantle). Note that this chemical trend is extended to refractory lherzolites and harzburgites in which CaO < 2.5%, Al_2O_3 < 3% and for sufficiently refractory compositions the anhydrous subsolidus mineralogy may be olivine + orthopyroxene + spinel, i.e., all CaO is dissolved in olivine and orthopyroxene, and clinopyroxene is not present as an additional phase.

The methodical study of the subsolidus mineralogy and melting behavior of these three compositions provides a basis for inferences on the nature of the asthenosphere and lithosphere that is summarized in the following sections. There are parallel studies of similar compositions by other workers that are broadly consistent although there are differences in detail. The studies described herein all used sintered oxide mixes or glass as starting materials. The use of crushed rocks or mineral mixes by many workers has introduced experimental difficulties in disequilibrium melting and persistence of original phase compositions (Falloon et al., 1999; Falloon et al., 2001) that are very difficult to eliminate.

The "Hawaiian pyrolite" (enriched mantle) has been studied most intensively for the roles of (C-H-O) in influencing melting and as representative of a suitable source (in incompatible elements particularly) for intraplate basalts. The Tinaquillo lherzolite composition is particularly relevant for "second-stage" melting or continuous melt extraction in the MOR setting.

The volatile-absent (C + H–free) solidi for the three lherzolite compositions (Fig. 1) differ by 50–70 °C at a given pressure due principally to differences in Na/Ca, K/Na, and Ti/Al

between the compositions. These differences expand the low-pressure plagioclase lherzolite stability field to high pressure for the more fertile compositions (note the comparison in Figure 1 with the simple systems CaO-MgO-Al_2O_3-SiO_2 [CMAS] and Na_2O-MgO-Al_2O_3-SiO_2 [NMAS]) and thus displace the "cusp" at the intersection of the subsolidus plagioclase-out boundary and the solidus. Another way to understand the differences in volatile-absent solidus temperature is to note that the plagioclase at the solidus of Hawaiian pyrolite at 1 GPa is ~An_{50} (anorthite$_{50}$albite$_{50}$), for MOR pyrolite it is An_{65}, and for Tinaquillo lherzolite it is $An_{75–80}$. In terms of adiabatic upwelling of mantle lherzolite, if the mantle potential temperature is 1280 °C, enriched compositions such as Hawaiian pyrolite begin melting at ~1.7 GPa (spinel lherzolite), in MOR pyrolite at ~1.3 GPa (plagioclase lherzolite), and in Tinaquillo lherzolite at 0.9 GPa (plagioclase lherzolite). If the mantle potential temperature is 1450 °C, melting begins in the three compositions at from 3.4 GPa (garnet lherzolite) in the enriched composition to 2.6 GPa (spinel lherzolite) in the depleted lherzolite composition. Thus solidus temperatures along an adiabat can be intersected over ~25 km depth range if there are small differences in incompatible-element and minor-element (Ti, Na) contents of lherzolite. The sensitivity of solidus temperature to composition is a reason to avoid use of average lherzolite solidus temperature estimations (McKenzie and Bickle, 1988; Hirschmann, 2000) in discussions of the genesis of particular magma types. The same point is well demonstrated in the progress from CMAS to NCMAS and NCMASF (Na_2O-CaO-MgO-Al_2O_3-SiO_2-FeO) systems summarized in Presnall et al. (2002), which emphasizes shift both in solidus temperatures and in near-solidus melt compositions with Na«Mg and Fe«Mg variation.

The (C + H)-absent melting relations are most closely approached in the genesis of MORB and in the formation of lithosphere at mid-ocean ridges and in other settings where assumptions of *complete* melt extraction during upwelling or diapirism would predict residues that are (C + H)-free. However, if melt extraction is not complete, e.g., if there is 1%–2% retained melt, it is difficult to entirely eliminate (C + H) from mantle sources and from influencing the melting process.

The Role of H_2O

Intraplate magmas and the lherzolitic xenoliths that many contain demonstrate significant roles for water and for carbon dioxide in intraplate magmatism. Pargasitic amphibole is observed as a minor phase, and occasionally as a major phase, in mantle-derived lherzolites, so it has been inferred that even very small quantities of water would lead to crystallization of accessory phlogopite or pargasite in fertile mantle. These observations led directly to experimental study of melting relationships of pargasite-bearing lherzolite (pyrolite + H_2O).

However, other experimental studies in which large amounts of water were incorporated into olivine and pyroxenes under particular conditions (Bai and Kohlstedt, 1992) led to an alternative view that, particularly in MORB source regions, the necessary water could be incorporated in lherzolite in nominally anhydrous minerals (olivine, pyroxenes, garnet) and H_2O could be treated as an incompatible component in dilute solid solution

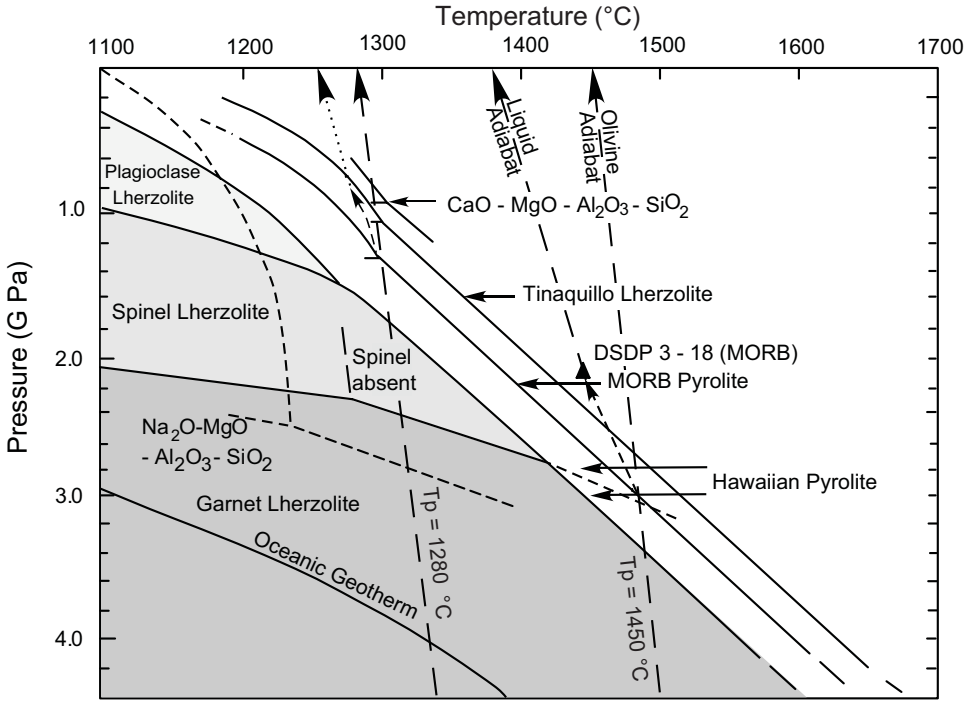

Figure 1. Experimentally determined solidi for Hawaiian pyrolite, mid-ocean ridge basalt (MORB) pyrolite, and Tinaquillo lherzolite compositions and stability fields for plagioclase, spinel, and garnet-lherzolite mineralogy for the Hawaiian pyrolite composition. Solidi are from sources cited in the text. Adiabats for mantle potential temperatures of 1280 °C and 1450 °C are shown, with a subsolidus adiabatic gradient of 10 °C/GPa and a liquid adiabat of 30 °C/GPa. The solid triangle is the inferred depth for magma segregation of MORB picrite DSDP (Deep Sea Drilling Program) 3–18 (2 GPa, 1430 °C) from Green et al., 1979. Solidi for the simple systems CaO-MgO-Al_2O_3-SiO_2 and Na_2O-MgO-Al_2O_3-SiO_2 are illustrated.

and as having little effect on solidus temperatures (Braun et al., 2000; Danushevsky et al., 2000; Presnall et al., 2002). Estimates of the water content of MORB-source mantle range from 100 ppm to 450 ppm (Michael, 1988), and other volatiles include CO_2 (a minimum of 50–100 ppm), fluorine, and sulfur (Presnall et al., 2002; Saal et al., 2002), all of which influence the presence or absence of a complex fluid at subsolidus temperature and determine the solidus temperature.

It thus becomes of critical importance to determine the equilibrium partitioning of water among olivine, pyroxenes, pargasite, phlogopite, and basaltic melts. Berry et al. (2004) have carefully investigated the mechanism of H_2O (OH^-) incorporation in olivine and conclude that olivine may contain up to 30 ppm H_2O under equilibrium conditions in the upper mantle (spinel lherzolite). They find maximum water contents in olivine in the higher-pressure garnet lherzolite mineralogy to be ~100 ppm. The results are also consistent with analytical data for natural olivines from spinel and garnet peridotites (Bell and Rossman, 1992; Kurosawa et al., 1997). Evidence on H_2O contents of orthopyroxene and clinopyroxene is equivocal, but assuming that orthopyroxene and clinopyroxene contain five and ten times the olivine concentration, respectively (Bell and Rossman, 1992; Ingrin and Skogby, 2000; Hauri et al., 2004), ~100 ppm is the maximum water content in "nominally anhydrous minerals" in fertile spinel lherzolite, and there may be higher but as yet uncertain contents in garnet lherzolite. These maximum values are achieved for high water activity, and the issues of presence or absence of fluid or melt or of hydrous phases such as pargasite or phlogopite at such levels of water activity must be considered. Using 100 ppm H_2O (max.) in the minerals of spinel lherzolite, if the MORB mantle contains 200 ppm H_2O, at subsolidus conditions at less than 3 GPa it will contain ~0.6% pargasitic amphibole. At pressures greater than that of pargasite breakdown (>3 GPa) and in the presence of carbon, MORB mantle would contain ~100 ppm H_2O in a complex (C-H-O and other volatiles) fluid phase at subsolidus conditions and ~0.03% melt (with ~30% H_2O) at the fluid-saturated solidus (~1050 °C, 3 GPa). Above the 3 GPa solidus, water contents in olivine and pyroxenes would decrease with increases in melt fraction and decreases in the water content of the melt phase (Hauri et al., 2004).

The role of carbon in magma genesis is simpler in one sense, because it has not been argued that carbon forms a dilute solid solution in mantle olivine, pyroxenes, and garnet (Keppler et al., 2003). Thus at low pressures carbon is present as CO_2-rich fluid inclusions, which are almost ubiquitous in spinel lherzolite xenoliths. However, at pressures between 1.5 and 2 GPa, carbonation reactions such as (olivine + diopside + CO_2 → enstatite + dolomite) lead to stabilization of dolomite as a stable subsolidus phase in the lower part of the lithosphere. Melting at pressures greater than that of the carbonation reaction produces sodic dolomitic carbonatite melts at temperatures below the silicate solidus. However, above the silicate solidus the carbonate dissolves in the silicate melt, modifying the melt toward more melilititic compositions (Wyllie, 1987; Wallace and Green, 1988; Falloon and Green, 1989; Dalton and Presnall, 1998).

The preceding scenario is applicable if the mantle is sufficiently oxidized, but the presence of diamond and graphite in mantle samples is evidence that this is not always the case. At lower oxygen fugacities, rather than (H_2O + CO_2) fluids, graphite (diamond) coexists with H_2O-rich fluids, or the fluid phase may consist of (H_2O + CH_4), with other volatile species (Green et al., 1987). Thus it became necessary to examine natural mantle samples for evidence of their oxidation state and to examine the stability of pargasite, carbonate, and graphite or diamond and the melting of mantle lherzolite under different oxygen fugacity conditions.

The Role of Oxidation State

The oxidation and reduction reactions involving iron are usually used as a sensor for mantle oxidation state, with particular reference to the Fe/FeO (iron/wüstite or IW) reaction. Oxidation reactions involving Fe (and Cr, Mn, Ni, etc.) and those involving carbon (CH_4, C, CO_2) have very different slopes in *P-T* space. A magma formed in equilibrium with diamond (or a fluid or magma precipitating diamond at high pressure) may be reduced in terms of Fe^{3+}/Fe^{2+} (at IW + 1 to 2 log units, for example) but will contain dissolved carbon as $(CO_3)^=$ and hydrogen as $(OH)^-$. On moving toward the Earth's surface at high temperature and decreasing pressure, the internal redox exchange and rapidly decreasing carbon solubility (between 2 GPa and 1 GPa) lead to fluid saturation and loss of a reduced CH_4 component in the degassing fluid, with accompanying oxidation of Fe in the silicate melt.

To understand mantle melting and lithosphere-asthenosphere relations it is thus necessary first to study lherzolite melting under controlled and different oxygen fugacity (fO_2) conditions and second to examine natural basalts and mantle samples for evidence of appropriate redox conditions.

Within the piston-cylinder apparatus using talc as pressure medium and graphite heater sleeves, the fO_2 conditions are close to IW + 2–4 log units in the 1–4 GPa pressure range (cf. early work in which Fe_2O_3 and FeO in experimental charges were measured [Green and Ringwood, 1967a,b]). The double-capsule method, with the outer capsule containing a more oxidizing or more reducing oxygen buffer, has also been used, in particular for the study of Hawaiian pyrolite + (C-H-O) at fO_2 = IW + 1–2 log units using a (tungsten carbide + tungsten oxide) buffer with graphite (Taylor and Green, 1988).

Most primitive magmas contain chrome-rich or aluminous spinels as early-formed microphenocrysts, and the magnetite solid solution component of the spinel acts as an fO_2 sensor. Spinels from MORB show lower fO_2 (IW + 3 log units) than Hawaiian olivine tholeiites (IW + 4 log units) and island arc magmas (IW + 5–6 log units) (Ballhaus et al., 1990).

Integrated Model for Intraplate Mantle

The preceding discussion provides the background against which the studies of Table 1 were undertaken. From this work an integrated model for the intraplate lithosphere and asthenosphere is presented in Figure 2 (from Green and Falloon, 1998). The preceding discussion has emphasized that carbon, hydrogen contents, and oxidation state exercise significant effects on the stability of minor phases, on the presence of a fluid, and on a *P-T* field for carbonatite melt and an incipient silicate melting regime. In presenting Figure 2, choices are made that H_2O contents in the lithosphere do not normally exceed those that can be retained in pargasite, i.e., a maximum of ~4000 ppm in fertile lherzolite but less in refractory compositions. Similarly, a specific model of fO_2 variation is presented, with fO_2 decreasing with increasing depth. If lithosphere at 60–100 km depth has lower fO_2 (≤IW + 2 log units), carbonate is not stable and graphite may be present. If portions of the mantle, e.g., suspended old subducted slabs or deep continental (cratonic) lithosphere, are more oxidized (fO_2 ≥ IW + 3 log units), carbonatite melt may persist deeper than 100 km in these deep oxidized volumes, and the silicate solidus (base of the incipient melting region) will continue to deeper levels at 400–500 °C below the (C + H)-absent solidus (the boundary of the major melting regime).

It is important to note that the incipient melting regime contains small melt fractions in equilibrium with garnet at depths below 70–90 km, 1150–1450 °C. The question of the mobility of this melt by porous flow is an open one, but its high level of dissolved volatiles ($H_2O + CO_2$) and its incompatible-element-enriched and strongly silica-undersaturated character will favor mobility (Minarik and Watson, 1995; Faul 2001). As a mobile ~1% melt, it will infiltrate along the geotherm as opposed to adiabatic upwelling (or ascend faster than adiabatic upwelling of the bulk lherzolite). However, for the intraplate geotherm illustrated, such melt will partially freeze at the intersection with the silicate solidus (~90 km), with enrichment in modal pargasite and possibly clinopyroxene. Carbonatite melt released at ~90 km will ascend further to crystallize at ~75 km as dolomite for the geotherm illustrated or, for a high geotherm, will intersect the decarbonation reaction at ~65 km with formation of clinopyroxene-enriched lherzolite to wehrlite and released CO_2-rich fluid (Green and Wallace, 1988; Yaxley et al., 1991). The model of Figure 2 predicts an intraplate asthenosphere that is fractionating over time, with the lower part of the asthenosphere becoming depleted in incompatible elements by loss of a mobile, fluid-enriched olivine melilitite to olivine nephelinite melt. Complementary to this deep asthenosphere depletion, the melt may metasomatize the lithosphere with two distinctive steps, pargasite enrichment (olivine nephelinite metasomatism) at ~90 km and carbonatite metasomatism at ~65 km. Alternatively, the migrating melt may be trapped in the uppermost asthenosphere at depths of around 90–100 km (Green, 1971; Green and Liebermann, 1976), producing a geochemical and rheological layering within the asthenosphere.

To further quantify the model of Figure 2 it is possible to contour the incipient melting regime for melt fraction and to

TABLE 1. LISTING OF RELATED EXPERIMENTAL STUDIES IN MANTLE MELTING AND MAGMA GENESIS SUMMARIZING THE INVESTIGATION OF THE EFFECTS OF (C + H + O) VOLATILES

Peridotite melting with (C + H + O)	Reference
Hawaiian pyrolite + H_2O (water-saturated)	Green (1973b)
Hawaiian pyrolite + 0.3% H_2O (water-undersaturated)	Green (1973b)
MORB pyrolite + H_2O (saturated and undersaturated)	Niida and Green (1999)
Tinaquillo lherzolite + H_2O (saturated and undersaturated)	Wallace and Green (1991)
K-enriched lherzolite + H_2O (saturated and undersaturated)	Mengel and Green (1989)
Hawaiian pyrolite + CO_2 + H_2O (fluid-undersaturated)	Wallace and Green (1988)
	Green and Wallace (1988)
Hawaiian pyrolite + CO_2 (carbonate-bearing lherzolite)	Falloon and Green (1989)
Hawaiian pyrolite + CO_2 + H_2O (fluid-saturated)	Falloon and Green (1990)
Hawaiian pyrolite + (C + H + O) at fO_2 = IW + 1 log unit (effectively Hawaiian pyrolite + CH_4 + H_2O)	Taylor and Green (1988)
Hawaiian pyrolite + (C+H+O+S) with controlled fO_2 and fS_2	Odling (1989)
Liquidus studies of intraplate magmas with (C + H + O)	
Alkali olivine basalt + H_2O	Green and Hibberson (1970)
Olivine-rich basanite + H_2O (+ CO_2)	Green (1973a)
Olivine nephelinite +H_2O	Bultitude and Green (1968)
Olivine melilitite + CO_2 + H_2O	Brey and Green (1975, 1976, 1977)
Olivine leucitite + H_2O	Edgar et al. (1976)
Olivine leucitite + CO_2 + H_2O	Ryabchikov and Green (1978)
Olivine lamproite + H_2O + CH_4 + F	Foley (1989)
Sodic-dolomitic carbonatite + H_2O	Sweeney et al. (1995)

Notes: This is not a comprehensive list of significant experimental studies on peridotite melting but rather a list of the sequential and related studies at Australian National University and the University of Tasmania, which are used to derive Figure 2 and the quantitative melting models of Figure 3A and B. fO_2—oxygen fugacities; fS_2—sulfur fugacities.

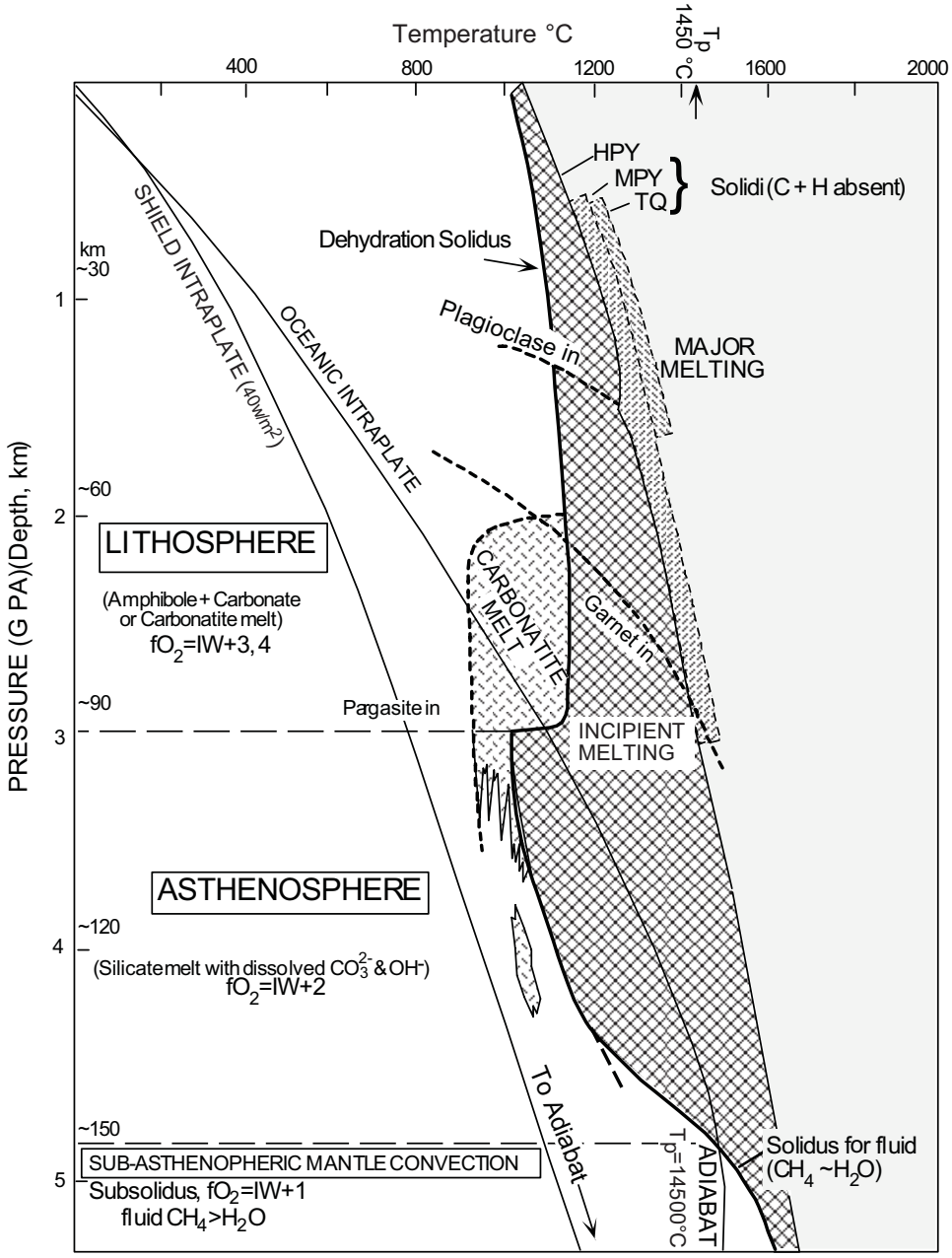

Figure 2. Application of the experimentally determined melting relationships for pyrolite and pyrolite + (C + H + O) to present a model for the intraplate lithosphere, asthenosphere, and subasthenospheric mantle. The oceanic intraplate geotherm represents a geothermal gradient equally appropriate for old oceanic crust and young continental crust. It is this geotherm that necessarily traverses the carbonatite stability field and incipient melting regime for the pyrolite compositions provided that the mantle $fO_2 \geq$ IW + 2 log units (IW—iron/wüstite or Fe/FeO reaction). Attention is drawn to the petrological base of the lithosphere, defined by the high-pressure pargasite breakdown and silicate solidus at ~95 km. The lower boundary of the asthenosphere (incipient melting regime along the geotherm) is drawn arbitrarily at ~150 km as the intersection of a mantle adiabat of potential temperature T_p = 1,450 °C with the pyrolite–(C + H + O) solidus for fO_2 = IW + 1 log unit. Below that depth a fluid with $CH_4 \geq H_2O$ is present, but there is no silicate melt unless fO_2 > IW + 1 log unit (i.e., a more oxidized region of the mantle). The carbonatite melt at more than 95 km and T < 1,000 °C is represented as present or absent depending on local variations in fO_2. That is, if $fO_2 \geq$ IW + 3 log units, carbonatite melt ± H_2O fluid (rather than graphite [diamond] + H_2O fluid) will be present. The shield intraplate geotherm does not intersect the silicate solidus and would meet the mantle adiabat at ~250 km. The implication is that there is no region of incipient melting for such geotherms. This geotherm can intersect the carbonatite solidus only if parts of the deep Archaean mantle are oxidized ($fO_2 \geq$ IW + 3 log units) and carbonate is present (from Green and Falloon, 1998). HPY—Hawaiian pyrolite; MPY—MORB pyrolite; TQ—Tinaquillo lherzolite.

estimate the melt fraction produced at the dehydration solidus (pargasite lherzolite solidus) if we assume a water content for the asthenospheric mantle. In taking this step it is emphasized that the melt component in the incipient melting regime is potentially mobile, the lithospheric plates are in motion, and lithospheric thinning and mantle upwelling are continuous, so any representation such as those in Figure 3A and B are "snapshots" of intraplate lithosphere. In Figure 3B the inferred conditions of the genesis and fluid contents of alkali olivine basalt (Green and Hibberson, 1970), olivine-rich basanite (Green, 1973a), olivine nephelinite (Green, 1973a), olivine melilitite (Brey and Green, 1977; Frey et al., 1978), and olivine leucitite (Ryabchikov and Green 1978; Foley, 1989) are illustrated for a fertile lherzolite composition containing ~1000 ppm H_2O, 400 ppm CO_2.

The melting behavior of peridotite + (C-H-O) suggests that in magmas produced from the upper mantle we might expect to see the more voluminous magmas as products of adiabatic upwelling and melt characteristics determined in the "major melting regime." These products are characteristic of mid-ocean ridges, back-arc basins, and "hotspots." Products from the incipient melting regime are seen in intraplate settings, including rift locations implying limited crustal thinning and lithospheric upwelling. It may also be expected that effects from the incipient melting regime are detectable in the major melting regime

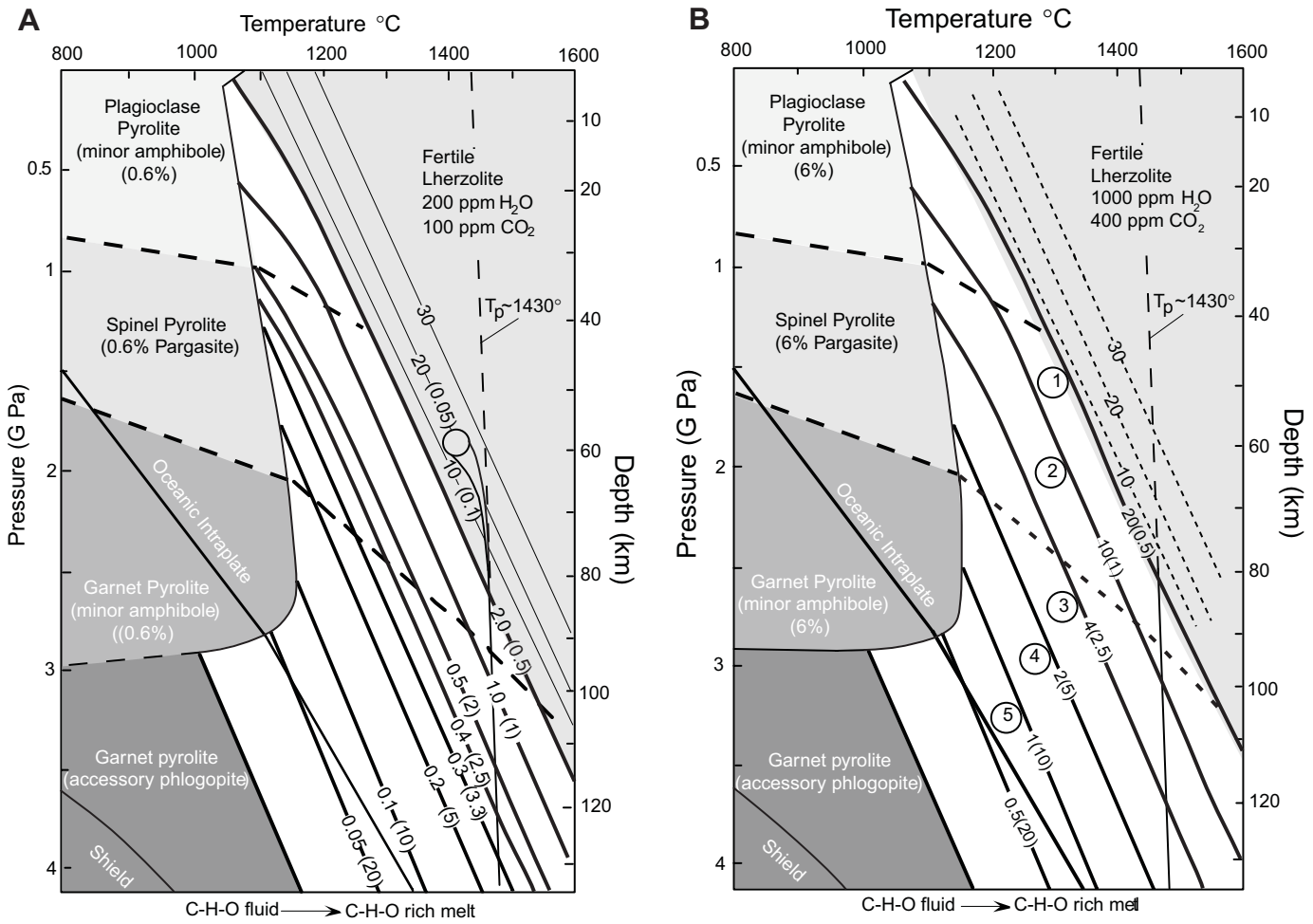

Figure 3. The incipient melting regime of Figure 2 may be contoured for melt fraction using information on the depression of the liquidus temperature by amount of dissolved water (Fig. 2; Green et al., 2001). The role of CO_2 is very pressure-dependent, with very low solubility at low pressures (<1 GPa) but solubility of ~10% CO_2 in olivine melilitite at 3 GPa with liquidus depression of ~100 °C (Brey and Green, 1977). Panels A and B of Figure 3 do not distinguish the carbonatite melt and carbonate stability fields of Figure 2 but address the C-H-O complexity by focusing on the water content and its role in entering pargasite at $P < 3$ GPa and entering a silicate melt phase (with dissolved $(CO_3)^=$ in the incipient and major melting regimes. In panel A it is assumed that ~100 ppm water is held in olivine and pyroxenes in equilibrium with pargasite or with a water-rich melt at near-solidus conditions. Contours are marked with melt fraction and dissolved water content (bracketed figures), and at large melt fractions melt contours are little different from the volatile-free melt contours (panel B), as dissolved water contents are very low. The separation of mid-ocean ridge picrites at ~60 km, 1430 °C is illustrated. In panel B the melt contours are drawn for ~1000 ppm H_2O, 400 ppm CO_2, approximating the source composition for intraplate magmas (see text). The conditions for magma segregation of (1) olivine basalts (transitional between olivine tholeiites and alkali olivine basalts), (2) alkali olivine basalts, (3) olivine-rich basanites, (4) olivine nephelinites, and (5) olivine melilitites or olivine leucitites are indicated. Note that (3), (4), and (5) are generated with residual garnet. Updated from Green and Liebermann (1976).

(mid-ocean ridge settings, etc.) as variations in depletion and addition of a fluid-enriched mobile component, effectively producing source compositions appropriate to D-MORB to E-MORB that are related by depletion or enrichment of a small melt fraction (<2% melt). Migration of melt from the incipient melting regime confers a "garnet signature" of REE relative abundances on regions affected by either depletion (HREE-enriched) or enrichment (LREE-enriched) by the migratory melt (Green, 1971; Green and Liebermann, 1976; McKenzie and Bickle, 1988; Faul, 2001; Presnall et al., 2002).

INTRAPLATE BASALTS (EXCLUDING "HOTSPOTS")

The "basalt tetrahedron" (Yoder and Tilley, 1962) is a convenient way of presenting the maximum amount of relevant chemical information on the major-element composition of both magmas and mantle sources in a format that allows visualization of liquid compositions lying on intersections of liquidus-phase surfaces. All major and minor elements of basaltic compositions, with the exception of TiO_2 and P_2O_5 (extracted in calculation of the molecular normative "end-members" as

rutile and apatite), are captured in the plotting components of the modified basalt tetrahedron (Green, 1971; Falloon et al., 1988), i.e., (jadeite + Ca-tschermak's silicate + leucite) + (diopside + hedenbergite) + (olivine [forsterite + fayalite]) + quartz. Within the tetrahedron, planes of silica saturation (hypersthene + plagioclase + diopside) and critical silica undersaturation (olivine + plagioclase + diopside) are readily identified, and extremely silica-undersaturated compositions have negative (quartz) and lie outside the tetrahedron.

In Figure 4 we have plotted the experimentally determined partial melting trends for Hawaiian pyrolite composition at pressures from 0.5 to 3.0 GPa under (C + H)-absent conditions and for the MM3 lherzolite composition at 1 and 1.5 GPa (MM3 lherzolite is a composition similar to Hawaiian pyrolite in major elements, including Ca/Al but with lower Cr/Cr + Al, influencing principally the composition of residual spinel at moderate degrees of melting [Falloon et al., 1999; Green et al., 2004]). At 0.5 and 1 GPa, plagioclase is a subsolidus phase in both volatile-free compositions and their melting relationships are similar, with the more fertile Hawaiian pyrolite producing more silica-undersaturated melts (nepheline normative) at near-solidus conditions. The "cusps" at plagioclase disappearance and clinopyroxene disappearance from the residue are clearly seen in the melting trends. At 1.5 GPa, melting is of the spinel lherzolite assemblages and the melts derived from Hawaiian pyrolite are more alkali-rich and silica-undersaturated and have higher Ca/Al (normative diopside) ratios than those from MM3. The differences are in part related to Na/Ca in pyroxene and plagioclase (Presnall et al., 2002) and to Cr/Al ratios in spinel (Green et al., 2004) particularly at the point of clinopyroxene disappearance. Thus the Cr # of spinel at clinopyroxene disappearance in Hawaiian pyrolite is 60, whereas it is ~30 in the MM3 and MOR pyrolite compositions (Green et al., 2004).

We have also plotted the field of mantle xenolith-bearing intraplate magmas (of Mg # >70) on the projections and the individual compositions of xenolith-bearing magmas from the southeast Australian Tertiary basalt province (Frey et al., 1978), for which the authors defined conditions of partial melting and melt fraction assuming a source composition close to Hawaiian pyrolite composition. The melt fractions defined were from ~4% at 2.5–3 GPa (olivine melilitite, olivine nephelinite) to 20%–25% melting at 1.5–1.0 GPa (olivine tholeiite). The more undersaturated melts separated from garnet lherzolite residue at temperatures below the volatile-free solidus and require significant dissolved $(CO_3)^{=}$ and $(OH^{-})^{-}$ for their genesis; they lie within the incipient melting regime of Figures 2 and 3. On the other hand, the compositions of higher melt fraction approach melts formed under (C + H)-absent conditions, i.e., they approach conditions within the major melting regime (Figs. 2 and 3).

The petrological model for intraplate magmatism envisages asthenosphere and basal lithosphere enriched over time by a migratory fluid-rich melt of olivine melilitite to olivine nephelinite character. Tension within the lithosphere may enable the escape of small-volume, volatile-rich, extremely undersaturated magmas. Dissolved C-H-O fluids in such magmas begin degassing at P >1 GPa and facilitate both eruption and transport of mantle xenoliths. If the tensional regime leads to crust or lithosphere thinning, upwelling from asthenosphere and lower lithosphere will approach adiabatic behavior, yielding higher melt fractions with compositions determined by the depth and extent of partial melting. Geodynamic settings of limited crustal extension are probably conducive to triggering of individual ascending diapirs within the broad asthenospheric upwelling. The diapirs may generate larger central volcanoes (tholeiites, olivine basalts) within a volcanic province dominated by small eruptive vents of more silica–undersaturated character. This model is applied in both ocean and continental intraplate settings, including seamount volcanism, "leaky-transforms," and post-erosional-stage (Hawaiian Island chain) volcanism of "hotspots."

With low degrees of melting and high pressures of magma segregation, minor- and trace-element enrichments in the melts reflect the role of residual garnet. However, this LILE and LREE enrichment during partial melting to yield strongly silica-undersaturated magmas is additional to prior enrichment (mantle metasomatism) events and processes operating within the asthenosphere beneath continental crust or oceanic crust and lithosphere (Green, 1971; Frey et al., 1978).

HOTSPOT VOLCANISM

The Hawaiian volcanic chain is a well-documented example of "hotspot" volcanism, and the main shield-building stage, dominated by olivine tholeiite volcanism, is accepted as the key to understanding the source composition and melting conditions for the inferred Hawaiian mantle plume. In a previous paper (Green et al., 2001) we used data provided by Norman and Garcia (1999) on picrite compositions from six volcanoes, together with their olivine phenocryst compositions, to infer parental magmas and their eruption temperatures for the magmas. This study identified "primary" magmas with 14%–18% MgO and anhydrous liquidus temperatures of 1330–1410 °C (1 atm). There is widespread acceptance that primary magmas from "hotspots," including Iceland, Réunion, and Kerguelen, are indeed picritic and suggest liquidus temperatures at 1 atm of ≥1350 °C. However, the dissolved H_2O and CO_2 in Hawaiian quenched glasses cannot be ignored, particularly those from picritic glass collected from the seafloor (Garcia et al., 1989; Clague et al., 1991; Seaman et al., 2004; Stolper et al., 2004), and result in liquidus depression of 50 ± 20 °C. The recent results of the Hawaiian Scientific Drilling Project in sampling deeper parts of Mauna Kea tholeiitic cone confirm the importance of low-pressure degassing of H_2O fluid and also confirm that prior to degassing, glasses with ~8% MgO contain 0.6%–0.7% H_2O (low-SiO_2 group) or 0.5%–0.6% H_2O (high-SiO_2 group) (Seaman et al., 2004; Stolper et al., 2004). Water contents in picritic parent magmas crystallizing olivine of Mg # = 90 would be ~0.4% to 0.6%, producing liquidus depression of 60 ± 20 °C.

We can calculate a primary magma composition from glasses

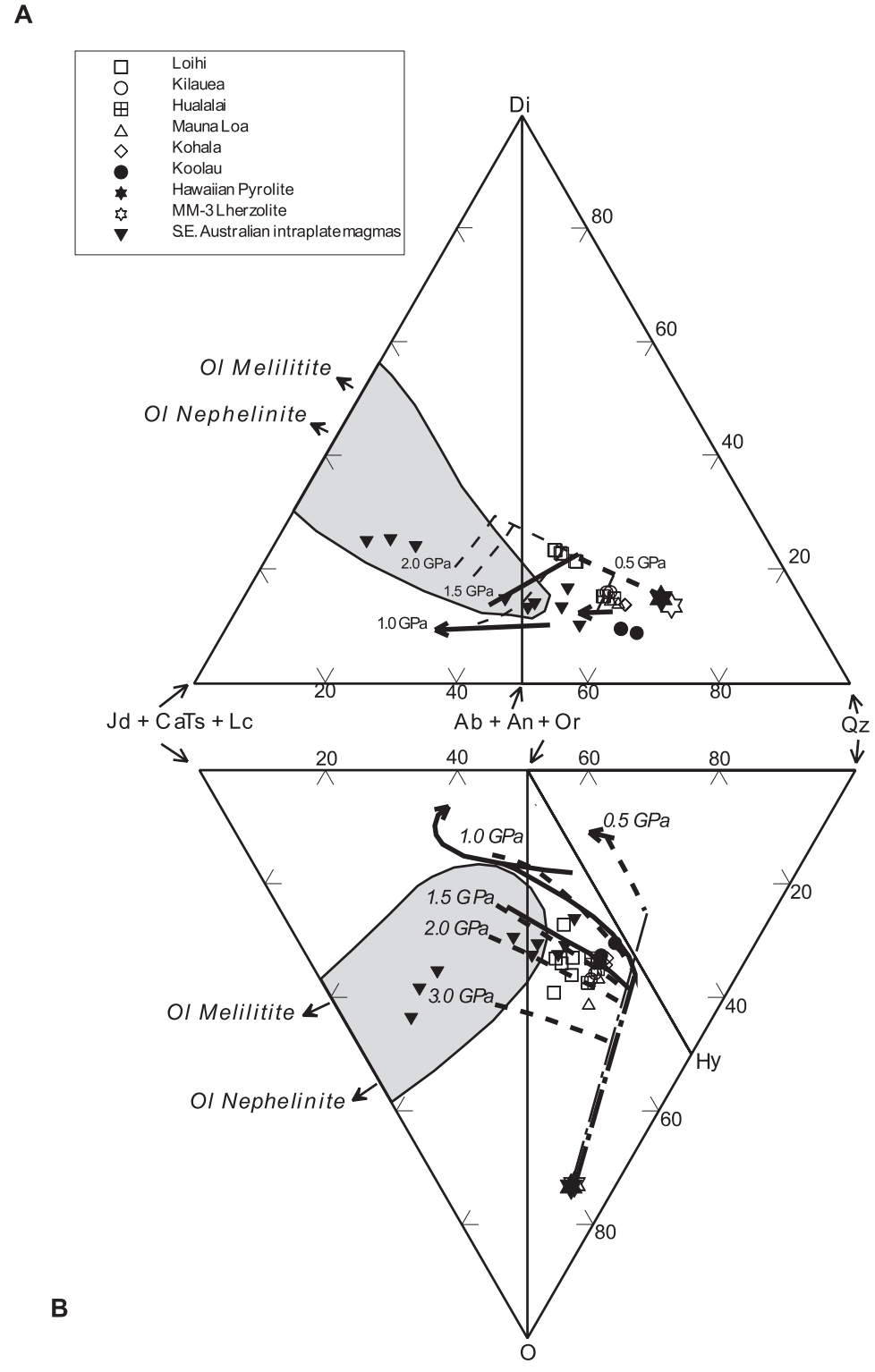

Figure 4. Projection of partial melting trends for Hawaiian pyrolite and MM3 lherzolite compositions, i.e., liquid compositions lying on lherzolite (olivine + orthopyroxene + clinopyroxene + spinel) and harzburgite (olivine + orthopyroxene + Cr spinel) cotectics for Hawaiian pyrolite (dashed curves, 0.5–2.0 GPa) and MM3 lherzolite (solid lines at 1 and 1.5 GPa only) compositions. Projections use the "basalt tetrahedron," (A) the projection from olivine (ol), and (B) the projection from diopside (di) (Falloon et al., 1988, 1999, 2001; Green and Falloon, 1998, 2001). Solid line with arrow is the locus of liquids in equilibrium with plagioclase lherzolite (olivine + orthopyroxene + clinopyroxene + plagioclase ± Cr spinel) at 1 GPa and 0.5 GPa; such liquids are low in normative diopside and olivine. The compositions of parental picritic magmas for Hawaiian volcanoes inferred by Green et al. (2001) are plotted (see legend) as well as inferred parental or primitive intraplate magmas from the southeast Australian Tertiary volcanic province (Frey et al., 1978). The shaded field encompasses the compositions of mantle xenolith-bearing, primitive magmas (i.e., Mg # > 70) and extends outside the tetrahedron to olivine nephelinite, olivine melilitite, olivine lamproite, and kimberlite magmas. Di—diopside; Ol—olivine; Jd—jadeite; Lc—leucite; Ab—albite; An—anorthite; Or—orthoclase; Qz—quartz; Hy—hypersthene.

that are saturated only with olivine (+ Cr-Al spinel) using the olivine-addition approach, by reference to the composition of the most magnesian olivine phenocryst observed (Green et al., 2001; Stolper et al., 2004) as the "end-point" of olivine addition. Alternatively, an assumption may be made as to source composition and residual olivine composition. Obviously if more magnesian olivine (Mg # = 91–92) is chosen, the postulated primary magma will be more olivine-rich. Also, from a given source the residual olivine composition will vary with % melting, e.g., primary picritic magma representing ~20% melting has residual olivine of Mg # = 90.5, but residue from 25% melting has olivine Mg # = 90.9.

In plotting magma compositions in the "basalt tetrahedron" as a means of constraining the conditions of partial melting, the projection from olivine into the plane (Jd + CaTs + Lc)-Di-Qz (Hy) is independent of olivine addition or subtraction. Analyzed glass or postulated picritic parent plot at the same point. In the projection from diopside onto the plane (Jd + CaTs + Lc)-Ol-Qz the addition or subtraction of olivine is the major determinant of whether postulated parent liquids lie on particular isobaric melting trends (Figs. 4 and 5). In previous sections we have discussed the composition of mantle-derived intraplate magmas and defined the melting trend from small melt fractions at high pressures (garnet lherzolite residue) to larger melt fractions at lower pressures (spinel lherzolite residue). The higher incompatible-element contents of Hawaiian tholeiitic magmas (in comparison with MORB) and their relative HREE depletion and LREE enrichment have been used by many authors to infer greater depths of melt segregation and derivation from garnet lherzolite. However, experimental studies of Kilauea tholeiitic picrite showed liquidus olivine followed by orthopyroxene at 1–1.5 GPa and orthopyroxene alone as liquidus phase at 1.8 GPa (Green and Ringwood, 1967b; Green, 1970; Wagner and Grove, 1998; Eggins, 1992a,b). Garnet appears at the liquidus only at ≥3.5 GPa.

Green et al. (2001) showed that the inferred primitive tholeiitic picrite liquids from Mauna Loa, Kilauea, Hualalai, Kohala, Loihi, and Koolau plot in compositional space in the basalt tetrahedron such that harzburgite (olivine + orthopyroxene + spinel) must be the residual mineralogy (Figs. 4 and 5). Expressed another way, these inferred picritic liquids do not lie on cotectics including plagioclase, clinopyroxene, or garnet, together with olivine, orthopyroxene, and spinel, at any pressure or temperature. In addition, liquidus spinels are Cr-rich, with Cr # > 60 (Norman and Garcia 1999), greater than values for MORB (20–60). Both the harzburgite residual mineralogy and the high Cr # of spinel show that, in terms of partial melting of fertile mantle lherzolite, Hawaiian picrites represent a relatively high degree of partial melting, greater than that of intraplate alkali olivine basalts, olivine basalts, or olivine tholeiites as exemplified by the Newer Volcanics of southeast Australia (Frey et al., 1978).

In Figure 4 we have plotted the partial melting trends for Hawaiian pyrolite from 0.5 to 3.5 GPa, together with the picrite inferred liquid compositions derived from Norman and Garcia (1999) and Green et al. (2001). In addition we have examined the compositions of magnesium-rich melt inclusions hosted in olivine in picrites as reported by Norman et al. (2002) for Loihi, Kilauea, Hualalai, Mauna Loa, and Koolau. Melt inclusions and matrix glass from Kilauea, Hualalai, and Mauna Loa form tight clusters (Fig. 5), including and slightly extending the "harzburgite

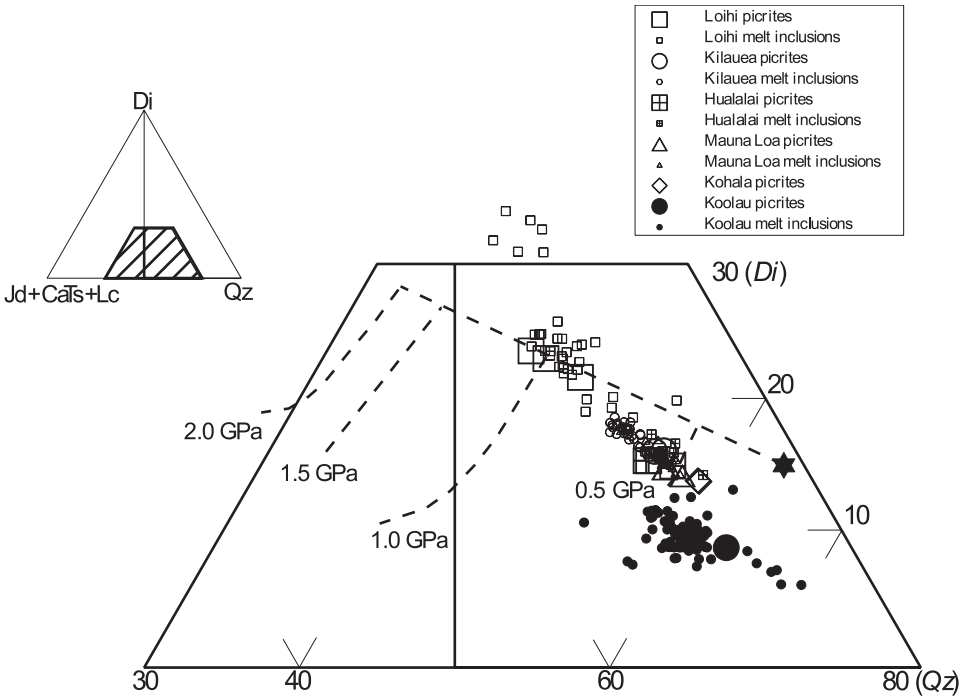

Figure 5. Enlargement of part of Figure 4A showing projected (from olivine) compositions of parental picrites from different Hawaiian volcanoes (Norman and Garcia, 1999; Green et al., 2001) together with melt inclusion compositions (>8% MgO only) from the same volcanoes (Norman et al., 2002). Melt inclusions overlap and extend the "harzburgite residue" trends defined for each volcano by the picrite compositions and, in the case of Loihi and Koolau, give a greater scatter, which is considered to reflect transient, trapped liquid compositions at olivine nucleation and growth sites coincident with resorption of wall-rock or magma mixing additions, e.g., clinopyroxene resorption for glasses with high-Ca/Al plagioclase resorption in Koolau low-diopside compositions. Di—diopside; Qz—quartz.

residue" trends defined by the picrite data (Green et al., 2001). The Loihi melt inclusions concentrate in a field paralleling the Loihi picrites but slightly displaced toward the diopside apex. There are a small number of melt inclusions with higher Ca/Al (trending to higher diopside contents) for which magma chamber processes of reaction, with clinopyroxene resorption, are possible (Kamenetsky et al., 1998). A small number of melt inclusions extend the harzburgite residue trend toward the quartz apex.

Similar observations apply to the melt inclusions from Koolau picrites. There is a dominant harzburgite trend that includes the two picrite compositions from Koolau (Norman and Garcia, 1999), but the harzburgite residue trend extends to both higher and lower normative quartz (Hy) in the dataset of melt inclusions in olivine.

The Hawaiian Scientific Drilling Project has sampled ~3 km of fresh tholeiitic basalts from the main cone-building phase of Mauna Kea volcano, much of the cone being of submarine lava flows. There is an extensive database of glass compositions from chilled pillow rims, chilled margins, and hyaloclastites. Stolper et al. (2004) have identified a dominant bimodal distribution of compositions, with the more primitive glasses having >7% MgO and comprising a low-SiO_2 group (48.5%–49% SiO_2) and a high-SiO_2 group (51%–52% SiO_2). We have plotted (Fig. 6) glasses with ≥8% MgO (low-SiO_2 group) and ≥7.25% MgO (high-SiO_2 group); in both cases these are glasses with Mg # > 54. The two groups are tightly clustered on a harzburgite residue trend in the projection from olivine but spread along olivine-control lines in the projection from diopside. Stolper et al. (2004) recognized the evolved character of both groups and used their tight coherence to calculate possible parental picrite by incrementally adding 20% and 22% olivine to the high-SiO_2 group and the low-SiO_2 group, respectively, to generate picritic compositions in equilibrium with olivine of Mg # = 90.5. These postulated parental compositions would lie on the 1.5 GPa and ~2.5 GPa olivine + orthopyroxene ± spinel cotectics for the Hawaiian pyrolite composition, respectively. The two harzburgite residue trends are not exactly colinear in the projection from olivine, with the high-SiO_2 group requiring a source with slightly higher Ca/Al. (Note also that isotopic and trace-element differences also preclude derivation of both groups from exactly the same source [Stolper et al., 2004.]) However, the relative positions of the two groups argues for a lower degree of melting for the low-SiO_2 group. It is thus possible to postulate derivation from very similar sources at 1.5–2 GPa, the low-SiO_2 picrite parent leaving harzburgite with olivine Mg # = 90, $P \approx 2$ GPa, and the high-SiO_2 picrite parent representing a higher melt fraction (+ ~5%), with residual harzburgite with olivine Mg # = 90.5, $P \approx 1.5$ GPa.

The dataset of glass compositions from Stolper et al. (2004) also includes three minor glass populations distinguished by the authors on the basis of major- and minor-element contents. One group represents eruptive material at ~1800 m depth (units 248–256) and is identified as having relatively high Ca/Al and high K_2O contents. Glasses with >7.25% MgO plot (Fig. 6) as a separate and coherent group in the basalt tetrahedron (projection from olivine), lying on the harzburgite residue trend for Hawaiian pyrolite composition but closer to the "cusp" at clinopyroxene-out. They overlap the Loihi picrites in this projection and imply a source with a higher Ca/Al ratio than the sources for the Mauna Kea low-SiO_2 and high-SiO_2 groups. Consistent with the conclusions (based on minor-element, trace-element and isotopic contents) of Stolper et al. (2004), this magma type is not simply related to either dominant magma type of Mauna Kea but represents a different (or chemically modified) source and a lower melt fraction, transitional toward the Hamakua olivine basalts (units 45 and 47; Baker et al., 1996; Rhodes, 1996).

A second "excursion" in compositions at ~2235 m depth (unit 288) is attributed to a smaller melt fraction than the dominant low-SiO_2 group (Stolper et al., 2004), and the variations in Na_2O, K_2O, and P_2O_5 within the unit (2280–2235 m below sea level) are consistent with ~30% difference in degree of partial melting, i.e., 20% to 14% or 10% to 7%. In the projection from olivine, this group of glasses lies at the low-degree-melt end of the low-SiO_2 group of glasses and extends the "harzburgite residue" trend to higher normative diopside. Note that the difficulty noted by Stolper et al. (2004) in that CaO increases rather than decreases with decreasing melt fraction (increasing Na_2O, K_2O, and P_2O_5), disappears if harzburgite rather than lherzolite is the residue from melting.

The third group of glasses, noted by Stolper et al. (2004) as high–(Ca + Al) glasses, occurs at several levels in the section but particularly at 2100 m. Projection of glass compositions with 7% MgO into the basalt tetrahedron (Fig. 6) suggests affinities with the more quartz-rich end of the low-SiO_2 group, but there is a suggestion of mixing toward the high-SiO_2 group. The values of K_2O, Na_2O, and P_2O_5 are consistent with mixing, but the CaO, Al_2O_3 values are higher, possibly because comparisons are made at different degrees of olivine fractionation.

Consideration of the Mauna Kea glass compositions in terms of patterns of melting of lherzolitic mantle leads to the firm conclusion that primitive or parental melts are related by crystal-liquid equilibria between picritic magmas and harzburgite (olivine and orthopyroxene ± Cr/Al spinel). This conclusion was also reached by Stolper et al. (2004).

A consistent picture for Hawaiian tholeiitic magmas emerges from the following:

1. Examination of picritic compositions in which the determination of olivine compositions permits estimation of parental or primitive magmas (Green et al., 2001).
2. Examination of melt inclusions in magnesian olivines (Norman et al., 2002), with the additional comment that some melt inclusion suites show evidence of magma-chamber processes of mineral resorption and reaction.
3. Examination of glass composition from ~3 km of tholeiitic shield volcano of Mauna Kea.

The data do *not* suggest a single-source composition, but rather the converse. However, they do argue that the composi-

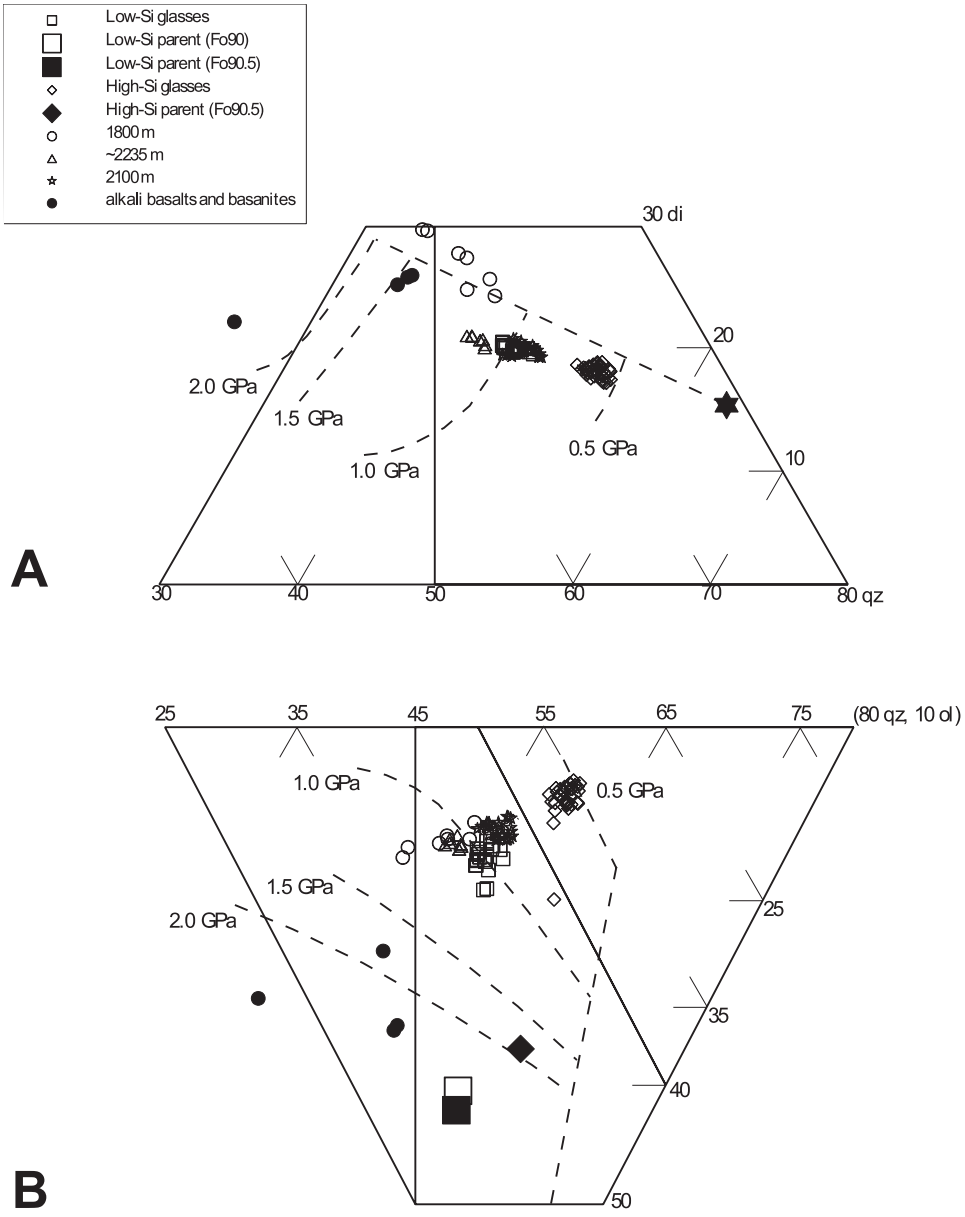

Figure 6. Enlargement of part of Figure 4A and B. Glasses plotted are from the Hawaiian Scientific Drilling Project (Rhodes, 1996; Baker et al., 1996; Stolper et al., 2004) sampling the main cone-building stage of Mauna Kea volcano. The "high-SiO_2" glasses plotted have >7.25% MgO, and the "low-SiO_2" group have >8% MgO. Glasses of distinctive composition identified at particular depth intervals in the core by Stolper et al. (2004) are also plotted, confirming their coherence as related compositions (see text). Three alkali olivine basalts and one basanite identified in the uppermost levels of the core are also plotted. In panel B are plotted the compositions of parent compositions for high- and low-SiO_2 groups estimated by Stolper et al. (2004) based on liquidus (residual) olivine of Mg # = 90.5, together with our equivalent estimates of parental liquids based on olivine of Mg # = 90 in the low-SiO_2 group and Mg # = 90.5 in the high-SiO_2 group. Di—diopside; Ol—olivine; Qz—quartz.

tions of primitive magmas of the main shield-building stage are determined by partial melting processes in which the only residual phases are olivine and orthopyroxene (and very minor spinel) and in which small variations in melt compositions faithfully reproduce different degrees of melting, i.e., different amounts of olivine + orthopyroxene entering the melt phase. The pressure at which the magma or harzburgite residue signature is determined is most readily estimated from the projection from diopside onto the base of the tetrahedron. The plotting position of parental or primitive magmas is determined by the extent of olivine addition, which we infer to derive the parental melt from the observed glass. This is well illustrated by the Mauna Kea high-SiO_2 and low-SiO_2 groups. Noting that olivine with Mg # = 90.5 was observed in Mauna Kea tholeiites (Baker et al., 1996), Stolper et al. (2004) calculated picritic parent liquids for both the high-SiO_2 and the low-SiO_2 groups, obtaining liquids with 17.4% MgO (low-SiO_2 group parent) and 15.95% MgO (high-SiO_2 group parent) using olivine with Mg # = 90.5 as the residue in each case. These estimates lie on the ~2.5 GPa and the 1.5 GPa melting trend for Hawaiian pyrolite, respectively. An alternative interpretation would result if the low-SiO_2 group represented a smaller melt fraction and Mg # = 90 rather than 90.5 was used to limit the olivine addition; the primitive or parent magma would then lie close to the 2 GPa melting trend. Our own calculations, using the PETROLOG program (Danyushevsky, 2001) and assuming fO_2 of QFM (quartz + fayalite + magnetite) + 0.5 log units, yield primitive magma for the low-SiO_2 group, with 15.6% MgO, olivine with Mg # = 90, and P ~ 2 GPa, and

primitive magma for the high-SiO_2 group, with 15.7% MgO, olivine with Mg # = 90.5, and $P \sim 1.5$ GPa.

Internal consistency in terms of olivine compositional shift in the "sources" would require the low-SiO_2 parent to represent ~20% melting and the high-SiO_2 parent to represent ~25% melting of lherzolitic sources similar to Hawaiian pyrolite or other mantle estimates with 3.5%–4% CaO, Al_2O_3.

Among the Mauna Kea glass compositions in the uppermost part of the section are three alkali olivine basalt (units 45 and 47) and one olivine basanite (unit 58) in which olivine appears to be the only phenocryst phase and rock compositions range from 8.21% MgO to 11.22% MgO. When plotted in the basalt tetrahedron (projection from olivine) these compositions lie on the 2 GPa melting trend for Hawaiian pyrolite composition and would be consistent with lherzolite residue. If K_2O and P_2O_5 are perfectly incompatible components, the relative abundances of the basanite, alkali olivine basalts, and tholeiites suggest that the more undersaturated magmas represent ~1/3 (basanite) and 1/2 (alkali olivine basalt) of the melt fraction represented by the low-SiO_2 tholeiitic picrites, assuming similar sources in terms of K_2O and P_2O_5 abundances. To summarize the Mauna Kea magmas, if a source composition similar to Hawaiian pyrolite is used, the olivine basanite (6%–7% melt), alkali olivine basalts (10% melt), unit 288 tholeiite (14% melt), low-SiO_2 group tholeiites (20% melt), and high-SiO_2 group tholeiites (25% melt) may be related by different degrees of partial melting, with the melt fraction increasing at lower pressures. These inferences from major-element compositions may be compared with trace-element and isotopic data, noting that heterogeneity in both these characteristics may reflect prior additions or depletions in incipient melt regime, with little effect on major-element and phase relationships.

However, although a coherent picture emerges relating tholeiitic magmatism (harzburgite residue, high melt fraction) and the waning magmatic-stage alkali olivine basalt to olivine basanite (lherzolite residue, low melt fraction), it is also apparent that source compositions vary in major element contents for each of the volcanoes. The projection from olivine demonstrates the importance of the composition (particularly in Ca/Al or normative diopside) of the source in defining the compositions of liquids lying on the harzburgite residue trend. Hawaiian pyrolite and MM3 composition with similar Ca/Al ratios define harzburgite residue trends appropriate for Loihi primitive magmas and Mauna Kea high-CaO and high-K_2O tholeiites, but are too high in Ca/Al for Mauna Loa, Kilauea, and the high-SiO_2 Mauna Kea tholeiites. The low-SiO_2 Mauna Kea tholeiites indicate slightly lower Ca/Al sources, and the Koolau picrite and melt inclusion data indicate a source that has a very low Ca/Al ratio, lower than that of MORB sources.

The combination of a common residual phase assemblage (harzburgite) together with divergent bulk "source compositions" as seen in the major-element systematics is reinforced by the trace-element and isotopic evidence. These data also show source variability between different volcanoes and between geochemically coherent units or groups of units within one volcano (Stolper et al., 2004, and references therein). The first aspect, the common harzburgite residue, may be seen as a direct and necessary consequence of the *P-T* conditions operating in the life cycle of a Hawaiian volcano. Thus effectively any peridotite composition, from harzburgite with <2% clinopyroxene and Cr-rich spinel to lherzolite with 15% clinopyroxene and Al-Cr spinel, will undergo partial melting at a lherzolite–C-H-O solidus and melt sufficiently to yield harzburgite (olivine + orthopyroxene + Cr-rich spinel) residue, but the melt fraction produced and its chemical signature in incompatible trace elements, isotopes, and even Ca/Al, Na/Ca ratios will directly reflect mantle heterogeneity and different precursor histories.

Causes of Mantle Heterogeneity in Intraplate and Hotspot Settings

There are two contrasting processes by which heterogeneity may be introduced in the upper mantle. The first is a direct consequence of the peridotite C-H-O solidus and the presence of an incipient melting regime at temperatures well within the *P-T* envelope defined by a mantle adiabat, whether the mantle potential temperature is as low as 1280 °C or as high as 1430 °C in the modern Earth. Migration of an incipient melt fraction (olivine nephelinite, olivine melilitite to kimberlite, or, if anomalously enriched in K_2O, olivine lamproite) along the geotherm produces depletion in one area and enrichment in incompatible elements in another area. Because these melts are enriched in dissolved $(OH)^-$ and $(C0_3)^=$ and have high Ca/Al ratios, the direction of metasomatism of "sources" is toward high Ca/Al and LILE enrichment. Carbonatite metasomatism is an extreme example of this type of metasomatism and is well documented for lithospheric samples (spinel lherzolite xenoliths). The rare earth elements show relative LREE depletion and HREE enrichment in mantle that has lost an incipient melt fraction (1%–2% melt) and LREE enrichment in mantle that has gained an incipient melt fraction. In terms of the asthenosphere-lithosphere model presented previously, upper mantle heterogeneity can arise from upward migration of an incipient melt producing LREE-depleted (D-MORB or N-MORB sources) garnet lherzolite at deeper levels in the asthenosphere and LREE-enriched (E-MORB sources) garnet lherzolite with higher Ca/Al at depths of around 100 km. Freezing of incipient melts into pargasite-bearing lherzolite at ~90–100 km will also metasomatize the base of the lithosphere.

The second distinctive process in generating heterogeneity in lherzolitic mantle arises from consideration of the fate of subducted slabs of oceanic crust and lithosphere. The buoyancy of such slabs relative to asthenospheric mantle will be determined by composition and temperature. Subducted oceanic crust recrystallizes to coesite eclogite at depths >50 km, and heating of mixed crust and mantle to approach ambient mantle tempera-

tures will cause melting of coesite eclogite to yield dacitic or rhyodacitic liquids, leaving residual garnet, pyroxene, and rutile (garnet pyroxenite or eclogite). These liquids are very reactive toward enclosing subsolidus peridotite, and theory, experiments, and example argue for their reaction and crystallization in the enclosing peridotite (Yaxley and Green, 1998; Green et al., 2001).

The result of this process is a distinctive refertilization of refractory harzburgite to lherzolite as the added component is a rhyodacitic or dacitic liquid enriched in incompatible elements (including a garnet-in-residue signature), which has high SiO_2, high Na/Ca, and very low Ca/Al. Resorption of dacitic liquid enriches the peridotite in garnet, orthopyroxene, and, to a lesser extent, clinopyroxene. This type of enrichment or refertilization of refractory harzburgite or lherzolite is advocated as the mechanism for generating the distinctive Koolau tholeiite source.

Summary—Hotspot Volcanism

The large amount of data in glass compositions from quenched submarine lavas, together with melt inclusion data from magnesian olivines and bulk rock + phenocryst relationships in tholeiitic picrite lavas, have been used to constrain and define the primitive or parental lava composition in the Hawaiian "hotspot" example. A remarkable consistency emerges in that primitive and parental magmas are picritic, with 14%–17% MgO and liquidus olivine of Mg # from 89 to 91.5. They plot in the "harzburgite residue" field defined by experimental melting studies on lherzolite compositions. Their volatile-free liquidus temperatures are 1345–1385 °C at 1 atm, but significant dissolved water $(OH)^-$ and carbon $(C0_3)^=$ lower pre-degassing liquidus temperatures by ~50 °C. It is also evident that the bulk compositions representing magma + residue (i.e., "source compositions") are variable, with trends toward both low Ca/Al (the eclogite melt or subduction signature) and high Ca/Al (the olivine melilite nephelinite or asthenospheric melt signature). Superimposed on the variable source composition signatures are differences in degree of partial melting shown by spread of compositions along the harzburgite residue vectors and most clearly revealed in the waning stages of volcanism, in which parental magmas trend toward alkali-olivine basalts and basanites. These magmas lie in lherzolite rather than harzburgite residue fields and are continuous with compositions of intraplate basalts (see previous section) and the posterosional basalts of Hawaii.

It is also possible to use the major-element compositions and systematics of lherzolite melting to infer the pressures at which the melt compositions are controlled by the phase relationships. As partial melts from lherzolite become more olivine-rich with increasing pressure and the most magnesian glass compositions are olivine-saturated at eruption, it is possible to add equilibrium olivine composition back into the liquids, up to the point at which the Mg # of liquidus olivine of the new bulk composition matches the Mg # of the most magnesian olivine observed. Because of the evidence for chemical heterogeneity among the sources for Hawaiian magmas, we do not consider that it is appropriate to assume a constant Mg # source for all melts. Also, melts and residues both become more magnesian with increasing degrees of melting, and this is particularly important if melt fractions of 5%–30% melting are indicated. We have therefore used the most magnesian olivine phenocryst compositions observed in a given magmatic unit to determine the end point of olivine-addition calculations and thus to *calculate parent liquid* compositions or inferred primary magmas. We have followed the methods of Green et al. (2001), using the data from their paper and the extensive glass composition data from Norman et al. (2002) for Mauna Loa, Kilauea, Koolau, and Loihi and from Stolper et al. (2004) for the Mauna Kea tholeiites (Hawaiian Scientific Drilling Project). The results are summarized in Table 2, confirming earlier conclusions that primary magmas are picritic, with 14%–17% MgO and anhydrous liquidus temperatures of 1345–1385 °C at 1 atm. The effect of dissolved water and CO_2, noted previously, lowers liquidus temperatures by ~50 °C, i.e., to 1295–1335 °C, or an average of 1315 °C. The pressures at which the primary magmas are formed are 1.3–2 GPa, implying the depths at which the harzburgite-residue trends are established, with the higher temperature and higher melt fraction magmas (Mauna Loa) indicating deeper levels of ~2 GPa (~70 km).

TABLE 2. CHARACTERISTICS OF PRIMARY MAGMAS INFERRED FROM GLASS AND PHENOCRYST COMPOSITIONS USING OLIVINE ADDITION AT fO_2 = QFM + 0.5 LOG UNITS AND THE PETROLOG PROGRAM

		Primary magmas		
Unit	MgO content	Liquidus olivine (most Mg-rich phenocryst)	Liquidus temperature (°C)	Inferred pressure for primary magma
Mauna Loa olivine tholeiite	17.0	Mg # = 91.3	1386	~2 GPa
Kilauea olivine tholeiite	16.6	Mg # = 90.7	1381	~2 GPa
Mauna Kea high-SiO_2 group	15.7	Mg # = 90.5	1367	~1.5 GPa
Mauna Kea low-SiO_2 group	15.6	Mg # = 90	1371	~2 GPa
Loihi	14.1	Mg # = 89	1343	~1.7 GPa
Koolau	14.2	Mg # = 89.2	1352	~1.3 GPa

Sources: PETROLOG program—Danyushevsky (2001); liquidus temperatures—Ford et al. (1983).
Notes: fO_2—oxygen fugacities; QFM—quartz + fayalite + magnetite.

MID-OCEAN RIDGE BASALTS

Our principal purpose in this section is to examine the database of natural MORB glass compositions to identify the most primitive or parental glass compositions and infer their temperatures of eruption. We then use information from experimental studies of lherzolite melting to test whether these liquids are primary magmas, i.e., consistent with equilibrium with lherzolite or harzburgite residues at some pressure and temperature. We wish to evaluate alternative models for MORB petrogenesis. One model argues that characteristic MORB form by melt segregation from lherzolite residue at pressures near 1 GPa, specifically that mantle upwelling intersects the mantle solidus near the transition from plagioclase lherzolite to spinel lherzolite and that the compositions of primitive MORB are a consequence of phase relationships above the solidus approximately at or below 1 GPa. The magma compositions formed in this *P-T* range are olivine tholeiites with ~12% normative olivine. This model argues for a mantle potential temperature of ~1280 °C for genesis of typical MORB (McKenzie and Bickle, 1988). In careful application of melting studies in the systems CMAS, NCMAS, and NCMASF, Presnall et al. (2002) considered compositions of MORB glasses and a subset of glasses with Mg # ≥ 68. They believe that this subset are evolved rather than primary magmas and have crystallized olivine or olivine + plagioclase from parental magmas generated above the volatile-absent lherzolite solidus at 0.9–1.5 GPa.

Presnall et al. (2002) also envisaged addition of small-volume (<0.2%) carbonatitic to kimberlitic melts from deeper levels above the lherzolite + CO_2 solidus; the model resembles that of Figure 2, but does not include a significant role for H_2O or lower fO_2 conditions below subsolidus carbonate stability. Presnall et al. (2002) infer a mantle potential temperature of T_p = 1260 °C. In explanation of the variability of basaltic crustal thickness along mid-ocean ridges, they state that "calculations indicate that melt productivity changes from 0% to 24% for a change in T_p from 1240 to 1260°C, effectively producing a rapid increase to full crustal thickness or decrease to none."

Other workers have examined the crytallization of MORB with 8%–10% MgO and ~10% normative olivine and found olivine and trace spinel but not plagioclase as liquid phases at low pressure (Green et al., 1979). These liquids are not primary magmas but are derived from picritic primary magmas by olivine + trace spinel crystallization (O'Hara, 1968; Green et al., 1979; Stolper, 1980; Elthon and Scarfe, 1984; Falloon and Green, 1988). The inferred primary magmas have 13%–16% MgO and represent liquids derived from lherzolite to harzburgite residues at 1.5–2.5 GPa. These primary magmas require mantle potential temperatures up to ~1430 °C (Green and Falloon, 1998; Green et al., 2001), i.e., much higher than the estimates of 1280 °C or 1240–1260 °C noted earlier. In this model, temperature differences along the ridge axis (i.e., possibly due to heat loss during upwelling) may produce primary magmas at less than the maximum permitted by a mantle T_p~ 1430 °C and separating from residual lherzolite at <2 GPa. Also, the higher potential temperature and greater depth of separation of primary picritic magma offers the possibility of continued near-adiabatic upwelling of residual mantle, with the potential for separation of second-stage melts (Duncan and Green, 1987) in near-axial settings and for shallow, partially molten residual mantle acting as a region of melt mixing, melt reaction, and melt impregnation for ascending primary picrites. These factors produce liquids that may reach olivine + plagioclase ± clinopyroxene saturation at low pressures, yielding the characteristics emphasized by Presnall et al. (2002). The second approach, however, has deliberately sought the most Mg-rich glasses as a pointer to the highest-temperature magmas at the ridges. A common aspect of all these models is that liquid compositions are constrained by phase equilibria relationships at particular depths, and their chemical compositions will reflect these.

There is now a large database of analyses of glass compositions from dredged and drilled seafloor basalts from mid-ocean ridges. The overwhelming majority of these analyzed glasses (and thus the implied majority of mid-ocean ridge basalts) reflect the superimposition of low-pressure processes acting in shallow magma chambers or in conduits (channels, dikes, permeable cumulate chambers). The processes include crystallization, porous reactive flow and wall-rock reaction, magma mixing, etc. These processes collectively impart complex low-pressure signatures and evolved magma compositions to average MORB. It is possible to use models of low-pressure crystallization behavior to estimate parental magmas (Klein and Langmuir, 1987), but for our purpose in this paper—the estimation of mantle potential temperature beneath mid-ocean ridges and the identification of primary magmas for MORB petrogenesis—it is appropriate to select those glass compositions with >9.5% MgO, for which only olivine (+ trace Al-Cr spinel) crystallization has modified a primary magma composition as plagioclase is not a phenocryst or liquidus phase. We thus avoid back-calculation of crystal fractionation or reactive porous flow that includes plagioclase or pyroxenes as contributing phases. All of these glasses have olivine phenocrysts or microphenocrysts, usually with reported spinel microphenocrysts, but there are unfortunately few compositional data on these spinels or olivines. Green et al. (2001) used eight examples of such glasses (those with >9.0% MgO) for which olivine phenocryst compositions were available and were consistently more magnesian (Mg # = 91.5–92.1) than the liquidus olivine for the glass composition (Mg # = 86.9–89.9, calculated for fO_2 = FMQ (fayalite-magnetite-quartz oxygen buffer) – 0.5 log units). By incrementally adding olivine to the glass composition (using PETROLOG, from Danyushevsky, 2001) until its liquidus olivine matched the most magnesian olivine observed, Green et al. (2001) calculated inferred primary magma compositions. These were picritic, with 13.0%–15.6% MgO. In an earlier study, Green et al. (1979) had shown that one of these glasses, DSDP (Deep Sea Drilling Program) 3–18, with 10.1% MgO, is saturated with olivine to 1.2 GPa and then has calcic clinopyroxene as the liquidus phase

at higher pressures. Experiments with added orthopyroxene at 1.2 GPa showed that the liquid was far from orthopyroxene saturation at this pressure, but by addition of ~15% olivine to form a picritic tholeiite with 16% MgO, the picrite was saturated with olivine and orthopyroxene at 2 GPa, 1420–1430 °C.

In Figure 7 we have projected the glass and inferred primary magma compositions for these glasses and picrites into the basalt tetrahedron and compare them with the partial melting trends for the MORB pyrolite composition at 1.0–2.0 GPa. As the MORB pyrolite composition was based on DSDP3–18 (24%) and residual olivine (57.5%) orthopyroxene (18%) and spinel (0.5%) (Green et al., 1979, their Table 5), it is no surprise that the DSDP3–18 picrite plots on the harzburgite residue trend at the clinopyroxene-out intersection for 1.8 GPa (projection from olivine) and on the 2 GPa "olivine + orthopyroxene" cotectic in the projection from diopside (note that the experimental composition [mix E] had 17% added olivine and 16.7% MgO and that at 2 GPa olivine preceded orthopyroxene crystallization by ~10 °C. Thus an "olivine + orthopyroxene"-saturated picrite at 2 GPa would have ~16.0% MgO.) The fields of the eight glasses and picritic primary magmas fall on the lherzolite to harzburgite residue trends at pressures of ~1.7–2 GPa. It is clear that these liquids do *not* show a reequilibration toward plagioclase lherzolite at ~0.5 GPa (i.e., the uppermost mantle-crust boundary) or even toward lherzolite or harzburgite residue at this pressure (see projection from olivine). Similarly, the compositions of the liquids are not consistent with a "point and depth average" (McKenzie and Bickle, 1988) of melt increments derived along a T_p~ 1430 °C adiabat or a T_p~ 1280 °C adiabat even if some physical process could be envisaged for extracting, transporting in isolation, and remixing such "point and depth" increments. Physically, we would expect such porous flow increments to undergo reaction and reequilibration with the lherzolite matrix in an upwelling, permeable column of melt + crystals.

The major-element compositions of the primary melts, defined on the basis of glass and observed phenocryst compositions,

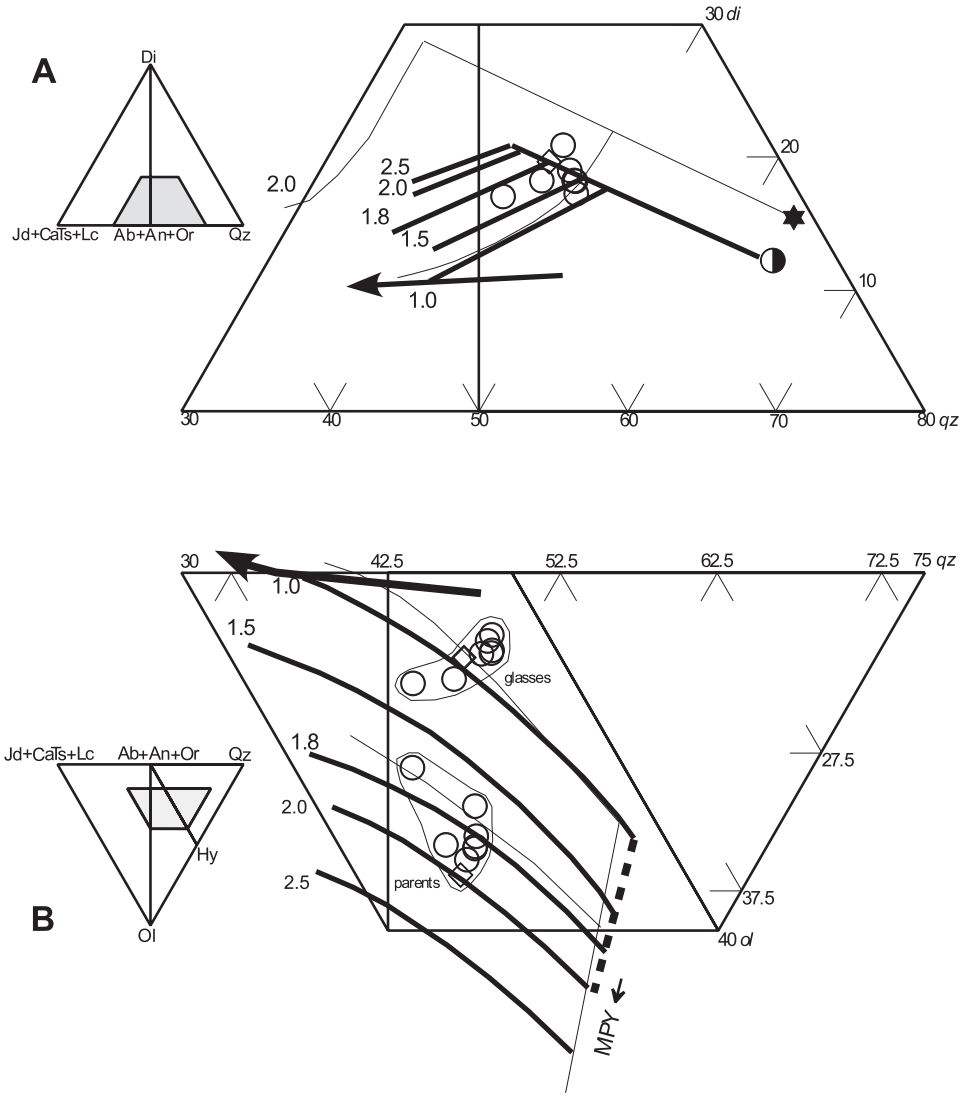

Figure 7. Projection of partial melting trends for the mid-ocean ridge (MOR) pyrolite composition (half-filled circle) from 1 GPa to 2.5 GPa and positions of eight MOR glass compositions and calculated parent compositions (Green et al., 2001). The parental compositions were calculated by incremental equilibrium olivine addition to match the olivine phenocrysts observed to be most Mg-rich. The MOR pyrolite cotectics are for plagioclase lherzolite at 1 GPa (olivine + orthopyroxene + clinopyroxene + plagioclase + Cr spinel), followed by increasing degree of melting, by a lherzolite trend (olivine + orthopyroxene + clinopyroxene+ Cr-Al spinel), and then by a harzburgite trend (ol + opx + Cr-spinel). At higher pressures plagioclase is absent at or below the solidus, and melting proceeds from spinel lherzolite to spinel harzburgite residues, with liquids becoming more alkalic at lower degrees of melting and increasingly olivine-rich with increasing pressure. The positions of the 1 GPa and 2 GPa cotectics from Hawaiian pyrolite (filled star) are shown for comparison. The solid arrow intersecting the 1 GPa MOR pyrolite lherzolite cotectic is the plagioclase lherzolite cotectic, with plagioclase becoming more sodic in the direction of the arrow. Di—diopside; Ol—olivine; Qz—quartz; MPY—MORB pyrolite.

apparently provide a clear signal of picritic melt + lherzolite to harzburgite residue at pressures of 1.7–2 GPa, i.e., depths of ~60–75 km, and temperatures at those depths of 1380–1430 °C (assuming liquid adiabat dT/dR = 30 °C/GPa. It is inferred that the picritic melts have reached the surface through dikes at shallow levels and dunite channels (Kelemen et al., 1992) at deeper levels, so their only chemical evolution during transit is one of precipitation of and reaction with olivine and minor spinel of limited variation in Mg #, i.e., between the liquidus value for the primary magmas and the more iron-rich olivines from the low-pressure olivine + liquid (+ trace spinel) phase field (cf. Green et al., 1979). The reasoning and information used in the analysis are silent on the prior, deeper (>1.7–2 GPa) processes of upwelling, melting, and melt migration and the incipient melt addition or extraction that gave rise to the bulk composition represented by "picrite melt + lherzolite or harzburgite residue" at the 1.7–2 GPa depth of magma segregation. In terms of a simple diapiric upwelling and emplacement at 1.7–2 GPa, the choice of a model mantle composition with 3%–4% CaO, Al_2O_3 determines that ~20% melting of picrite composition is required to eliminate residual clinopyroxene at ~2 GPa, 1420 °C.

We have examined our earlier conclusions based on the selected MgO-rich glass compositions for which there are olivine phenocryst compositions against the much larger dataset of mid-ocean ridge glass compositions. The database used is the Petrological Data Base of the Sea Floor (petdb.ldeo.columbia.edu). We identified 199 analyses of glass from ridge axis sites with >9.5% MgO, and 190 of these were complete, in terms of major-element determinations, for our purposes. The calculated liquidus temperatures (1 atm) using the geothermometer of Ford et al. (1983) and fO_2 = QFM – 5 log units are mostly in the range from 1225 to 1250 °C, and olivine compositions are within the range Mg # = 86–89 (with thirteen exceptions, of which one is outside the range Mg # = 85–90). We have not at this time attempted classification into E-MORB, N-MORB, or D-MORB, noting that definitive incompatible trace element data are commonly not available, but variations in K_2O, P_2O_5 indicate that the suite includes E-MORB as well as N-MORB (and probably D-MORB).

In Figure 8 we project all 190 compositions into the basalt tetrahedron and compare them with the partial melting cotectics for MORB pyrolite at 1–2.5 GPa. The data points are highly grouped around the 1–2 GPa lherzolite to harzburgite cotectics in the projection from olivine but around the 0.6 GPa to 1.3 GPa cotectics in the projection from diopside. Significantly, the compositions do *not* lie close to the olivine + orthopyroxene + clinopyroxene + plagioclase cotectic at 1.0 GPa for either MORB pyrolite or more fertile or refractory compositions. Instead they lie on the spinel lherzolite residue field or the spinel harzburgite field. A significant number (particularly from the Galapagos ridge and Mid-Atlantic Ridge) plot above (i.e., have higher Ca/Al) the harzburgite trend through the MORB pyrolite composition, implying that this estimate of asthenospheric mantle ("primitive modern mantle") is a little too low in Ca/Al (normative diopside:plagioclase).

In the projection from diopside, the tightly clustered dataset is suggestive of a sequence of liquids with lherzolite residue from <1.5 GPa to ~0.6 GPa, but note that this would imply that no olivine addition was required to reconstruct primary liquids, i.e., the source would have olivine of Mg # = 86–89. This inference is also not compatible with the olivine projection in which liquids from 0.6 GPa to 1.5 GPa would be displaced toward the quartz apex. However, if olivine is incrementally added to these glass compositions, in the projection from diopside the compositions will move toward higher-pressure olivine + orthopyroxene cotectics and the inferences from both projections will be mutually consistent. This is explored in more detail by examining some of the data from particular spreading centers.

In Figure 9 we plot twenty-one glass analyses (fourteen localities) from the East Pacific rise and eight from the Carlsberg ridge (two localities). The East Pacific rise samples fall in the lherzolite residue field and group around 1.5 GPa cotectic (projection from olivine) but ~1–1.2 GPa in the projection from diopside. Olivine addition back to liquidus (residual) olivine with Mg # = 91 moves the parental compositions to overlap the 1.5–1.8 GPa cotectics in both projections. Comparing the two ridge datasets, the phase equilibria suggest lower degrees of melting (lherzolite residue) and greater depth of magma segregation (~50–60 km) for the East Pacific rise and higher degrees of melting (close to that of clinopyroxene elimination) and shallower depths of magma segregation (~35 km) for the Carlsberg ridge samples. Liquidus temperatures for inferred parental magmas are 1300–1315 °C (East Pacific rise) and 1310–1315 °C (Carlsberg ridge). Attention is drawn to the TiO_2 and Na_2O contents of glasses from the two groups: 0.7% TiO_2, 1.7% Na_2O in Carlsberg ridge samples and 0.9%–1.1% TiO_2, 2.3%–2.5% Na_2O in East Pacific rise samples. These differences are consistent with higher degrees of melting at Carlsberg ridge (compare these with the olivine with Mg # = 91.5 and 91 used in calculating parental magmas for Carlsberg ridge and East Pacific rise samples, respectively).

The Galapagos ridge samples (Fig. 10) collectively group around the 1.5 GPa cotectic from lherzolite to harzburgite residue (projection from olivine). Incremental olivine addition to a common residual olivine (Mg # = 91.5) produces parental liquids crossing the 1.8 GPa cotectic and with liquidus temperatures (1 atm) of 1340–1380 °C (Fig. 12). An alternative approach is to note the natural grouping of the glasses in the projection from olivine and to observe that the three groups so defined could represent increasing degrees of melting at ~1.5 GPa, i.e., residues from olivine Mg # = 89.5 to olivine Mg # = 90.5. Liquidus temperatures range from ~1300 to 1320 °C.

The Mid-Atlantic Ridge glasses extend from <1 GPa to >2 GPa in the projection from olivine but from <1 GPa to 1.5 GPa in the projection from diopside (Fig. 11). No glasses lie close to the plagioclase-bearing cotectic at 1 GPa or lower pres-

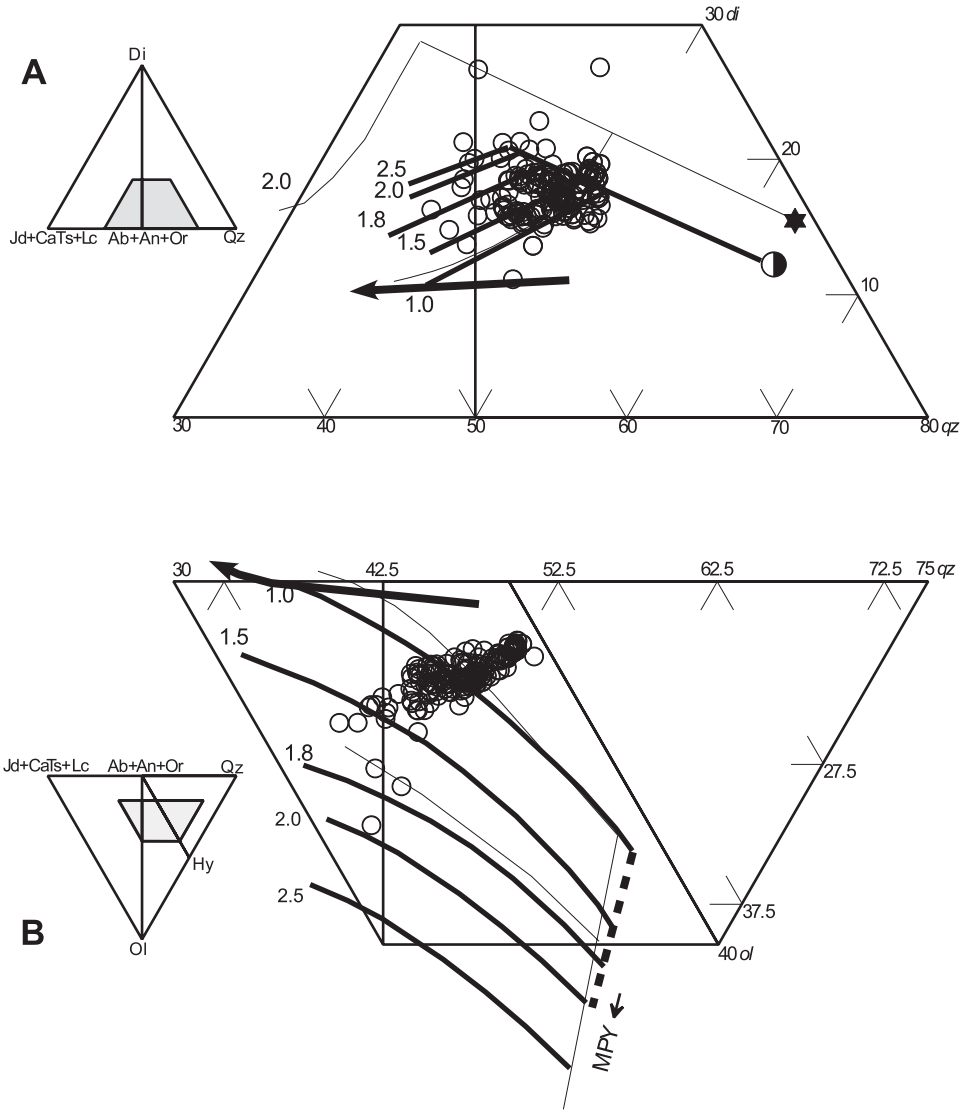

Figure 8. The same as Figure 7 but with ~190 glass compositions plotted from the ocean floor glass database (see text). The glasses have >9.5% MgO and were sampled from mid-ocean ridge locations. There is insufficient data to consistently distinguish enriched mid-ocean ridge basalts (MORB), depleted MORB, and normal MORB on the basis of incompatible element concentrations. Di—diopside; Ol—olivine; Qz—quartz; Hy—hypersthene; MPY—MORB pyrolite.

sures, but compositions spread from the harzburgite residue field into the lherzolite residue field. In Figure 12 we plot the Mg # of calculated liquidus olivines and liquidus temperatures (using PETROLOG, from Danyushevsky, 2001, and Ford et al., 1983) for each of the analyzed glasses. Liquidus temperatures are concentrated around 1220–1240 °C, but there is a surprising range of liquidus olivine compositions (Mg # = 86–89.5), indicating that only a very few of the glasses approach primitive liquids, i.e., liquidus olivine with Mg # ≥ 89. Some Mid-Atlantic Ridge glasses have olivine phenocrysts up to Mg # = 91.5 (Green et al., 2001) and we have arbitrarily chosen this composition as the end point of incremental olivine addition to derive "parental" liquids from the observed glasses. The calculated "parental" liquids have liquidus temperatures of 1300–1380 °C (Fig. 12). Examination of the data shows the existence of a subgroup of liquids with ~1 GPa olivine + orthopyroxene ± clinopyroxene + spinel saturation and liquidus temperatures of 1300–1320 °C. This subgroup includes several glasses with high Mg #, i.e., requiring little olivine addition, and others of lower Mg #, requiring more olivine addition. Also, those glasses that in the projection from olivine lie at positions with high normative diopside and low normative quartz and have liquidus olivines with Mg # = 86.5–88 require significant olivine addition, i.e., parental liquids with Mg # = 91.5 have liquidus temperatures of >1340 °C, <1380 °C; these are picritic magmas with >14% MgO, many with >15% MgO.

Finally, with reference to Mid-Atlantic Ridge magmatism, we refer to the picrites of Baffin Island and west Greenland, in which magnesian olivine phenocrysts and skeletal olivine have long been used as evidence for picritic rather than olivine tholeiitic parental magmas (Clarke, 1970; Francis, 1985). Yaxley et al. (2004) have examined host magmas and olivine-hosted melt

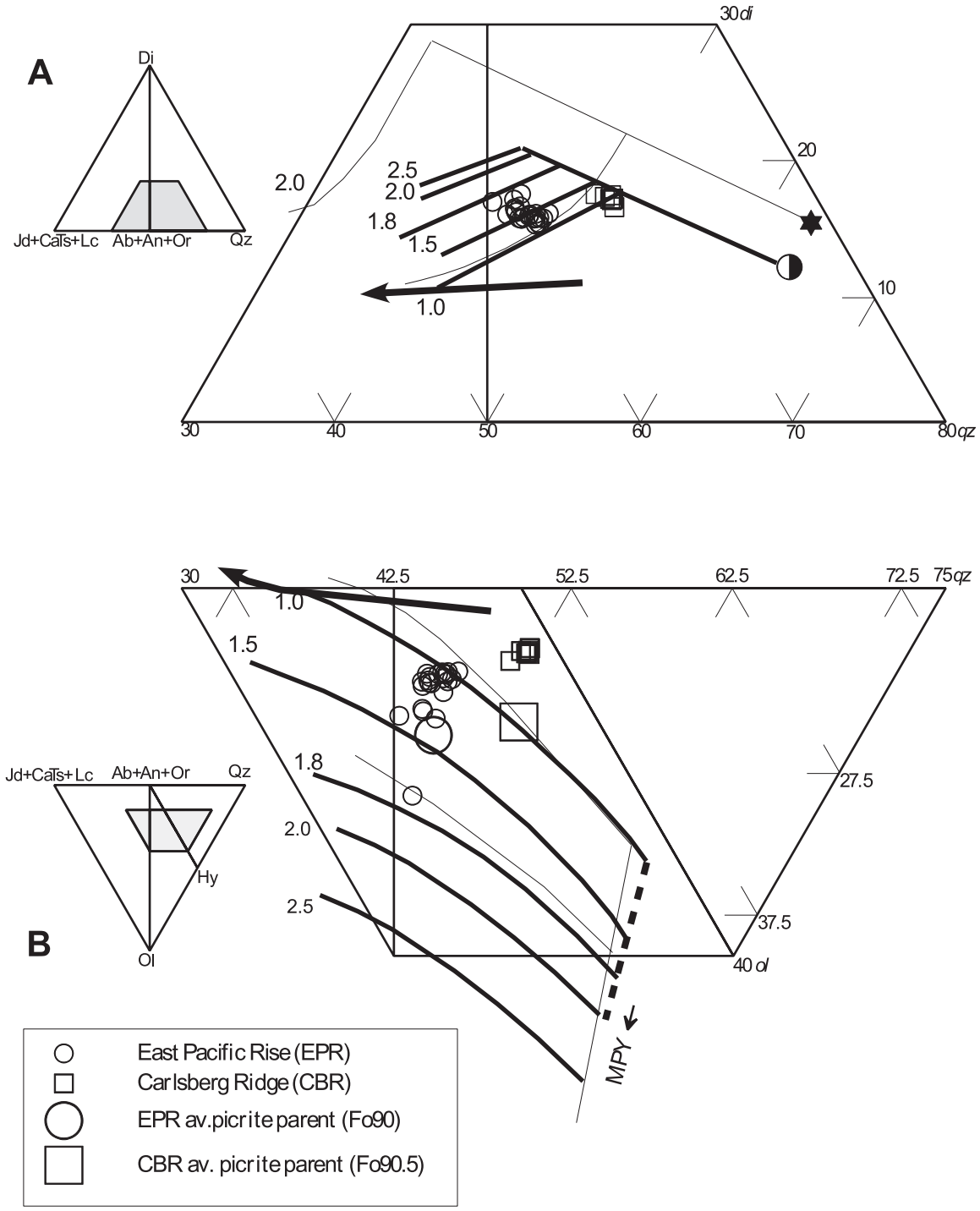

Figure 9. The same as Figure 7 but the glasses plotted are from the East Pacific rise and Carlsberg ridge spreading centers. The incremental addition of olivine up to liquidus olivine with Mg # = 90.5 produces parental liquids for the Carlsberg ridge overlying the 1 GPa cotectic in both projections, which is at or close to the lherzolite to harzburgite cusp, i.e., elimination of clinopyroxene from the residue. The East Pacific rise glasses lie in the lherzolite-residue field (1.5–1.8 GPa) in panel A but require olivine addition for consistency with these pressures in panel B. An average parent calculated for liquidus olivine with Mg # = 90 lies close to the 1.5 GPa cotectic in panel B. Di—diopside; Ol—olivine; Qz—quartz; Hy—hypersthene; MPY—MORB pyrolite.

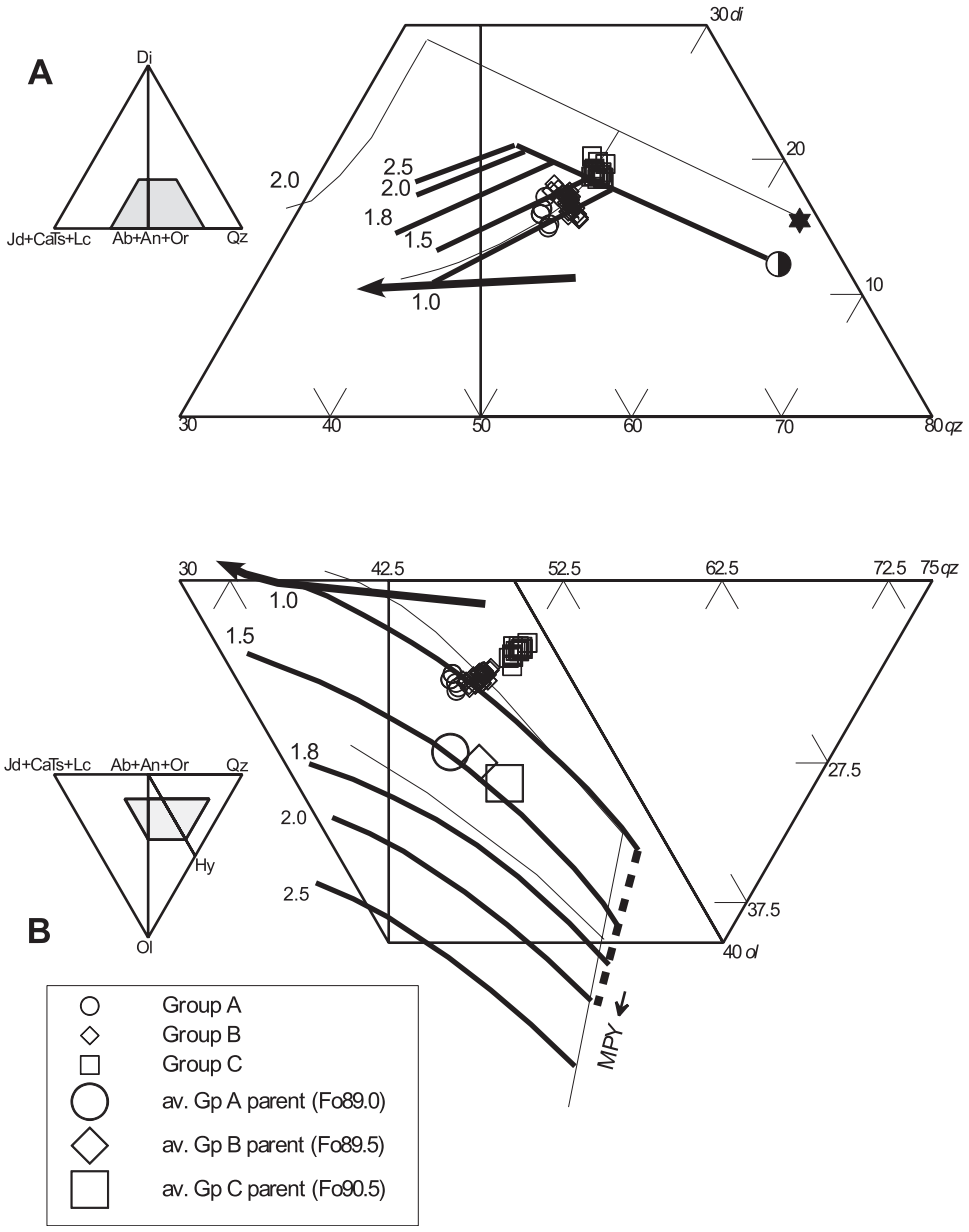

Figure 10. Same as Figure 7 but glasses from the Galapagos ridge are plotted. These glasses appear to fall into three groups. Groups A and B lie in the lherzolite-residue field at pressures around 1.3–1.5 GPa, with B consistent with higher degrees of melting. Group C are the most silica-rich and plot at the clinopyroxene-out cusp and ~1.5 GPa. Possible parent magmas for average glass of each group are calculated for olivine of Mg # = 89, Mg # = 89.5, and Mg # = 90.5 for A, B, and C, respectively. Using olivine of Mg # = 91.5 for all groups gives liquidus temperatures of 1340–1380 °C (1 atm), and liquids would plot at 1.8–2 GPa in panel B. Di—diopside; Ol—olivine; Qz—quartz; Hy—hypersthene; MPY—MORB pyrolite.

inclusions from Padloping Island and demonstrate olivine + Cr-Al spinel crystallization as the liquidus and near-liquidus phases. Robillard et al. (1992) and Yaxley et al. (2004) provide minor-element and trace-element data that identify the magmas as typical N-MORB with some slight enrichment in incompatible elements, trending toward E-MORB. Yaxley et al. (2004) demonstrate limited wall-rock reaction with the Archaean metamorphic terrane through which the picritic magmas have passed and note preferential recording of transient contaminated liquids encapsulated in growing olivine phenocrysts. This contamination is barely detectable in the chilled margin bulk compositions that may be used to estimate parental liquid compositions. Yaxley et al. (2004) provide five picrite analyses, two with 14%–14.6% MgO and three with 18.2%–21.4% MgO. They also provide information on compositions of olivine phenocrysts from Mg # = 85 to Mg # = 91, together with rare olivine with Mg # = 92.9 and maintaining a "high" (0.33%) CaO content, all of which is consistent with equilibrium with the enclosing magma. Spinels included in olivine have Cr # = 45–57, i.e., they are at the refractory, high–Cr # end of the MORB array (Dick and Fisher, 1984; Arai, 1987).

When projected into the basalt tetrahedron, the picrite compositions plot at the high normative diopside and low normative (Jd + CaTs + Lc) limit of the Mid-Atlantic Ridge field (Fig. 11) in the projection from olivine. They define a short "harzburgite residue" trend at pressures of 1.8–2.0 GPa but require a source

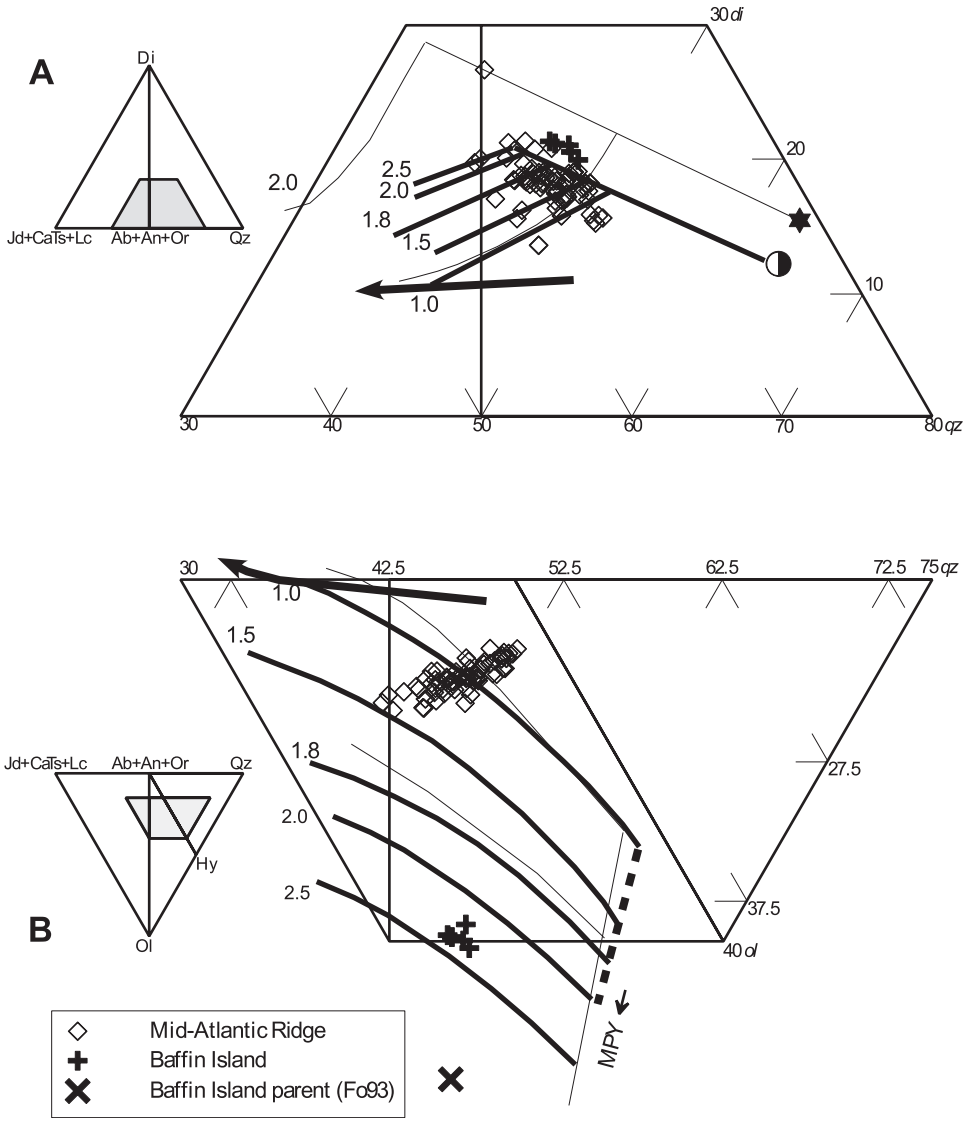

Figure 11. Same as Figure 7 but with glasses from mid-Atlantic ridge sites. In panel A glasses range from 1 GPa to >2 GPa, and most lie in the lherzolite-residue field, extending to harzburgite residue. The calculated parental picrites for Baffin Island (Yaxley et al., 2004) are plotted (**+**) for olivine of Mg # = 91. The calculated parent for olivine of Mg # = 93 (Yaxley et al., 2004) is also plotted (**x**).

with slightly higher Ca/Al than the MORB pyrolite composition (as noted previously for other Mid-Atlantic Ridge and Galapagos glasses). The position in the projection from diopside depends sensitively on the correct assessment of the liquid and liquidus olivine composition to be inferred from the rock and mineral compositions. In Figure 11 we have calculated (using PETROLOG, from Danyushevsky, 2001) liquid compositions from each picrite for liquidus olivine of Mg # = 91. This requires incremental addition of olivine (5%–7%) to two compositions and removal of olivine (6%–13%) from three compositions. The resulting estimates of parental liquids have 16.5%–17.0% MgO and calculated liquidus temperatures of 1377–1386 °C. These inferred picrite magma compositions project between the 2.0 and 2.5 GPa cotectics in the projection from diopside, i.e., consistent with inferences from the olivine projection. However, if liquidus olivine of Mg # = 92.9 is used, inferred parental melts have 21.2% and 22.1% MgO (Yaxley et al., 2004) and liquidus temperatures of ~1450 °C, but in the projection from diopside the liquid will plot on the olivine + orthopyroxene cotectic at >3 GPa. If the olivine of Mg # = 92.9 is typical of the most primitive magma, extremely high temperatures are indicated, but if in the demonstrable wall-rock reaction processes there is opportunity for local redox perturbation, these rare olivines may not be indicative of parental magma. We prefer the more conservative use of olivine of Mg # = 91 to infer parental picrites with liquidus temperature of ~1380 °C and MgO 16.7%.

The inferred parental magmas of the Baffin Island picrites lie at the high-temperature end of the spectrum of Mid-Atlantic Ridge glasses and inferred parental magmas. They are clearly of MORB affinity in terms of incompatible element abundance, i.e., they are a consequence of upwelling and partial melting of the type of mantle (? asthenospheric mantle or primitive modern mantle [PMM]) that is the source for worldwide MORB. However, because the evidence for picritic liquids has been clearly

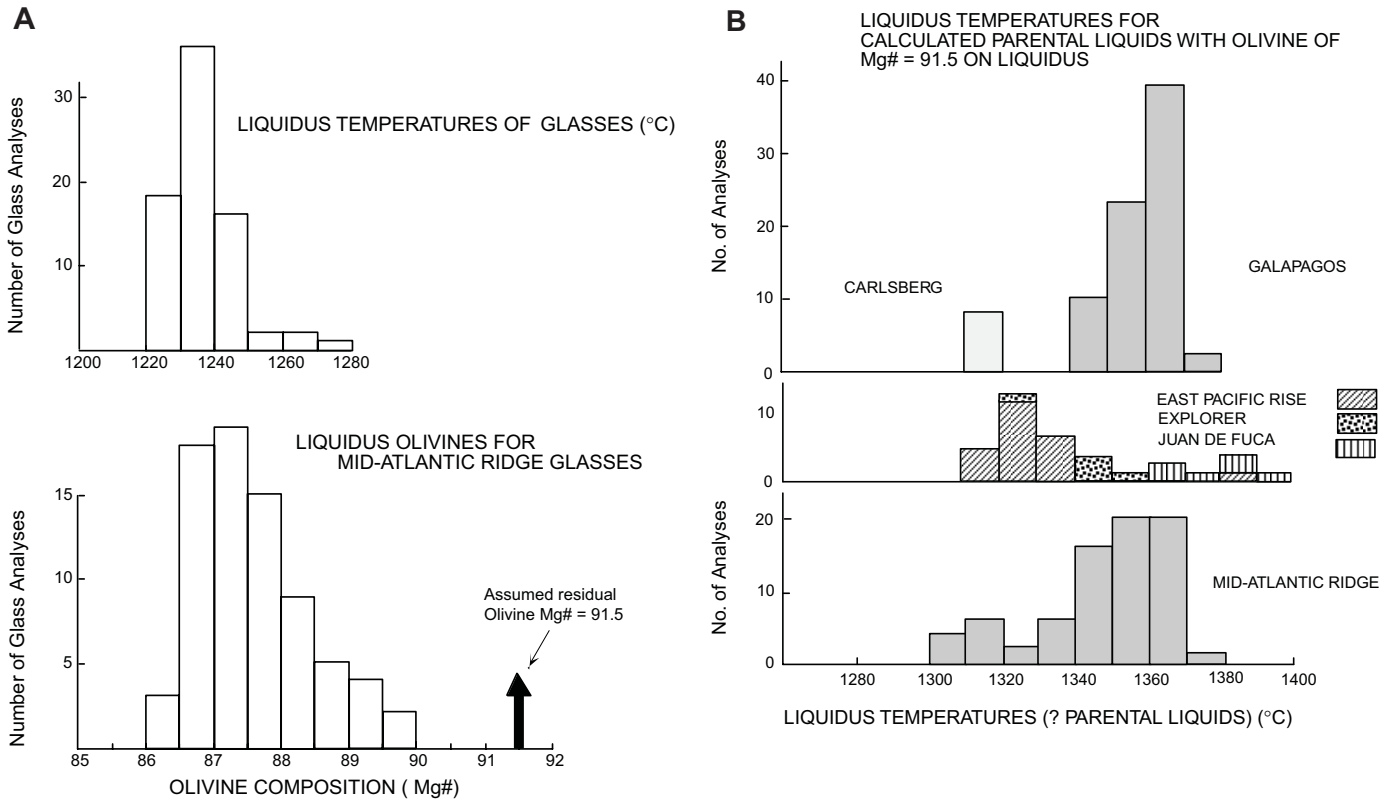

Figure 12. (A) The liquidus temperatures and compositions of liquidus olivines for mid-Atlantic ridge glasses with MgO ≥ 95% calculated using Petrolog (Danushevsky et al., 2000) (see text). (B) In the lowest diagram, the glasses plotted in panel A are individually recalculated (using PETROLOG) to a parent composition assuming olivine of Mg # = 91.5 on the liquidus. The liquidus temperatures of these parental or primitive picrites are plotted (1300–1380 °C). In the two diagrams in panel A, the same procedure is adopted for glasses from the other designated spreading centers.

presented in earlier work, the implied higher-than-normal temperatures have been attributed by some authors to the early stages of the "Iceland plume" and by others to a separate, no longer active, mantle "plume." The proposals advanced to explain MORB chemical signature in a postulated plume require the transfer of the high-temperature aspects of the hypothetical plume to normal MORB mantle (PMM) *without* transfer of the postulated plume geochemical signal.

Summary and Conclusions on MORB Petrogenesis

There is a robust inference that asthenospheric mantle, sampled on a worldwide basis by both collection of ocean floor peridotites (residues) and by MORB (partial melts), is lherzolitic in composition and close to estimates such as those for PMM (Sun and McDonough, 1989) or MORB pyrolite (Green et al., 1979). The experimental study of melting relationships of MORB pyrolite, MM3, and Tinaquillo lherzolite provides a detailed empirical database of residual phase and equilibrium liquid compositions against which natural glass (melt) compositions can be matched. The Petrological Data Base of the Sea Floor (petdb.ldeo.columbia.edu) provides a very large number of glass analyses from samples taken from mid-ocean ridge spreading centers. The great majority of these glasses are evolved along multiphase saturation surfaces (olivine + Cr-Al spinel ± plagioclase ± clinopyroxene) at low pressures, have liquidus temperatures <1250 °C and liquidus olivine compositions of Mg # < 89 (see also Presnall et al., 2002). There is a significant population of glass compositions with ≥9.5% MgO that crystallize olivine + (Cr-Al) spinel only for 20–30 °C from liquidus to plagioclase appearance at ≤0.1 GPa. Because our interest is in assessing the maximum temperatures of magmas and deducing mantle potential temperatures for asthenospheric mantle upwelling at mid-ocean ridges, we have examined these 190 high-MgO glasses for evidence of their conditions of origin.

None of the glasses with ≥9.5% MgO lies on or close to olivine (Mg # ≥ 89) + pyroxenes + plagioclase + Crspinel saturation at 1 GPa or lower pressures, i.e., they do not have compositions controlled by melt segregation from residual plagioclase lherzolite or by reactive porous flow through plagioclase lherzolite at or near the crust-mantle boundary or deeper levels. Although the transition from plagioclase to spinel lherzolite occurs over a significant pressure and temperature interval (Fig. 1; see also Presnall et al., 2002) the plagioclase at the solidus at higher

pressures (>1 GPa) is more sodic, and liquids in equilibrium with such sodic plagioclase become alkalic and remain with low normative diopside with increasing pressure from 1 to 1.5 GPa. The observed glasses with ≥9.5% MgO do not follow these compositional trends (Figs. 7–11). They lie in the field of spinel lherzolite (olivine + orthopyroxene + clinopyroxene + Al-Cr spinel) to harzburgite (olivine + orthopyroxene + Cr-Al spinel) residue, mostly at pressures of 1.5–2 GPa. There are variations between ridges and along ridges, suggesting that there are some locations with signatures of low pressure (1 GPa) and high degrees of melting (harzburgite residue, melt with low TiO_2, Na_2O and high Mg #) and other locations with higher pressures (2–2.2 GPa) and high degrees of melting (harzburgite residue, Cr-rich spinel). East Pacific rise samples indicate lower degrees of melting (1.5–1.8 GPa lherzolite residue, higher TiO_2, Na_2O in melts), whereas the Baffin Island picrites, displaying MORB minor-element and trace-element geochemistry, emplaced in the early stages of rifting between Baffin Island and Greenland, indicate high degrees of melting at ~2–2.2 GPa (harzburgite residue with Cr-rich spinel [Cr # = 50], low Na_2O and TiO_2 in melts).

The inferred pressure (depth) of magma segregation from lherzolitic to harzburgitic residue is derived from both projections (from diopside and from olivine) in the basalt tetrahedron but is most sensitively inferred from the diopside projection and relies on the correction for olivine crystallization applied to the glass analyses. As this correction is based on the liquidus olivine or residual olivine assumed for the parental magma, independent evidence for this is desirable either from phenocryst or from residual peridotite compositions. Also, if a range of pressures and degrees of partial melting (and possible fO_2) is appropriate, residual olivine for low melt fractions may be Mg # = 89.5 and for higher degrees of melting may be Mg # = 91.5. We have inferred depths of magma segregation from ~1 GPa to ~2.2 GPa and degrees of partial melting possibly from 10% to 25%. Liquids are picritic, with 13%–16% MgO, the higher MgO content being typical of the deeper levels of magma segregation. Magma liquidus temperatures (1 atm) range from ~1310 to 1380 °C, the lower-temperature magmas also indicating lower pressures. If we assume 30 °C/GPa for the picritic liquid adiabat (compare with an olivine adiabat of 10 °C/GPa) and make adjustment for latent heat of melting (10%–25% melting), the mantle potential temperatures indicated are ~1350 to 1450 °C.

These estimates are made assuming anhydrous magmas, but both N-MORB and particularly E-MORB contain small but significant H_2O and CO_2 contents (Danyushevsky et al., 2000; Saal et al., 2002). We have not been able to adequately sort the ~190 MORB glass analyses used into N-MORB, D-MORB, and E-MORB types as trace-element data are not always available. However, all three types are present and do not appear to correlate with either liquidus temperatures or depths of magma segregation. Maximum potential temperatures may be reduced by ~20–30 °C due to effects of water in lowering liquidus temperatures and lowering % melt contours (Fig. 3A and B).

The MORB pyrolite composition (Green et al., 1979) provides a satisfactory source composition for many primitive MOR picrites, but consideration of the larger population of glass analyses now available suggests a composition of modern asthenospheric mantle (PMM) with a Ca/Al ratio slightly higher than that of MORB pyrolite.

PRIMARY MAGMAS AND MANTLE POTENTIAL TEMPERATURES

Intraplate Magmatism

Intraplate magmatism, with its relatively high frequency of primitive, silica-undersaturated magmas containing high-pressure mantle xenoliths, is the major source of information on intraplate lithosphere and asthenosphere. In this paper we have summarized the evidence for a petrological lithosphere (subsolidus with respect to silicate melt) overlying asthenosphere in which there is a small, volatile-enriched and very silica-undersaturated melt in equilibrium with garnet lherzolite—the incipient melting regime of Figures 2 and 3. Extraction of magmas may occur directly from the incipient melting regime under conditions favored by deep tension fractures and high (C-H-O) volatile contents in magmas, i.e., magma degassing at high pressures, creating fluid-driven crack propagation. Significant lithospheric stretching and limited asthenospheric upwelling produces rift structures and volcanism of alkali-olivine basalt to olivine tholeiite character. Because of probable heat loss from small diapirs or plumes and the significant role of (C-H-O) volatiles in lowering liquidus temperatures of primitive magmas whose depth of origin can be constrained (Figs. 3 and 4), the study of intraplate magmas does little to constrain mantle potential temperatures in intraplate settings, i.e., they may be consistent with T_p~ 1300 °C or T_p~ 1450 °C. We infer that intraplate magmatism is a consequence of transient extensional events that, through limited asthenospheric upwelling, produce perturbed geotherms linking mantle adiabat and crust- or lithosphere-conductive geotherm. The source compositions involved in upwelling and magma production are characteristically enriched in volatiles and incompatible elements, and we should note that, beneath continents in particular, there are long time intervals and multievent histories that may contribute to melt migration (incipient melting regime) and metasomatism in both asthenosphere and lithosphere. Upwelling or heating of lithosphere may cause dehydration melting of pargasite or phlogopite + pargasite lherzolite at $R < 2.5$ GPa, further contributing to incompatible-element-enriched melts in the rifting environments. The particular trace- and minor-element characteristics of intraplate primitive magmas (LILE + LREE enrichment) are common to all intraplate settings, and although relative enrichments appropriate to residual garnet are enhanced in the melting process for low-degree, high-pressure melts, the presence of the enriched signature in the higher-degree melts (alkali olivine basalts,

olivine tholeiites) is indicative that it is also a source characteristic (i.e., "sources" are not chondritic or LREE-depleted).

Hotspot Magmatism

The main shield-building eruptive stage of the Hawaiian volcanoes defines the highest temperatures of the eruptive cycle yielding volatile-free liquidus temperatures at 1 atm of 1345–1385 °C. Significant dissolved volatiles ($CO_3^=$ and OH^- principally) lower pre-degassing temperatures by ~50 °C. The compositions of primitive glasses, i.e., glass compositions consistent with the most magnesian olivine phenocrysts observed (Mg # = 89 to Mg # = 91.3), are indicative of harzburgite residues. In addition, liquidus spinels have higher Cr # (>60) and are more oxidized than spinels of MORB. Mauna Loa, Mauna Kea "high-SiO_2 group," and Koolau tholeiitic picrites in particular have compositions that do not have clinopyroxene or garnet as liquidus phases coexisting with olivine, orthopyroxene, and Cr-rich spinel at any pressure. At the waning stages of volcanism and posterosional eruptions, magmas become richer in Na_2O, CaO, and Al_2O_3; plot in lherzolite residue fields and are indistinguishable from intraplate basalts of similar degrees of silica undersaturation.

We have also shown that source compositions defined by combining primitive melts + harzburgite residue are variable from volcano to volcano but distinctive for each volcano. Some trend toward low Ca/Al (Koolau trend) and others toward high Ca/Al (Loihi, Mauna Kea high-CaO, high-K_2O group), and it has been suggested that these contrasted trends are indicative of enrichment by dacitic melt (near-solidus melt from eclogite, i.e., a subduction signature) or by olivine melilite nephelinite melt (the peridotite incipient melt), respectively. Additional source inhomogeneity is present in Fe/Mg (Koolau is more Fe-rich than Kilauea or Mauna Loa) and in minor elements, trace elements, and isotopic signatures. An extensive literature confirms the greater isotopic and trace-element heterogeneity of Hawaiian "hotspot" magmas than MORB, and analysis of major-element compositions and phase relationship implications also shows clearly that this heterogeneity, including that of major and trace elements, is *not* a product of the final melt and residue reaction and melting process but is a product of previous history.

We have used the systematics of major-element compositions to infer depths of magma segregation, i.e., the condition at which olivine + orthopyroxene + Cr-Al spinel saturation occurs, of 1.3 GPa (Koolau) to 2 GPa (Mauna Loa, Kilauea, Mauna Kea low-SiO_2 group). The anhydrous liquidus temperatures for individual volcanoes (Table 2) may be extrapolated to their respective depths of magma segregation along liquid adiabats of 30 °C/GPa (McKenzie and Bickle, 1988). They must then be reduced by ~50 °C for effect of dissolved (C-H-O) and increased by an estimate for latent heat of melting to yield a point on the solid adiabat. The potential temperatures derived for the Hawaiian hotspot range from ~1400 °C (Mauna Loa) to 1350 °C (Loihi, Koolau).

Mid-Ocean Ridge Magmatism

The overwhelming majority of observed glass and inferred magma compositions at mid-ocean ridges are evolved liquids indicative of an environment in which eruption rates and volumes are sufficient to maintain high temperatures to crust-mantle boundary depths. These conditions are conducive to fractional crystallization, reactive porous flow, and wall-rock reaction. Magmas, cumulates, and residues are expected to show complexity around an overall trend toward low-pressure (<0.5 GPa) saturation in olivine (Mg # < 89) + clinopyroxene + plagioclase (An_{75}-An_{95}) saturation. Nevertheless, in seeking evidence of maximum temperatures and parental magmas at MOR settings, it is appropriate to extract any glass compositions with >9.5% MgO and, noting that such liquids crystallize olivine + Cr-Al spinel at their low-pressure liquidus, we may infer that such liquids have penetrated the uppermost mantle through dikes or dunite channels without low-pressure cooling and reaction with plagioclase or clinopyroxene-bearing peridotites or gabbros. A similar conclusion holds, for example, at Kilauea volcano, where the 1959–1960 eruption brought picritic magma from >60 km depth rapidly to surface eruption and only in later eruptive stages was it evident that mixing began between the deep-origin picrite and magmas in earlier, partly crystallized magma chambers or conduits. Both in the MOR and the Kilauean example, the MgO-rich liquids preserve their high-pressure melt and residue signature and may be used to infer pressures and temperatures of primary magma genesis.

The majority of glasses with >9.5% MgO have liquidus olivine of Mg # = 86.5–88, and incremental addition of olivine to take their liquidus olivine to Mg # = 91.5 gives picritic liquids with 14.5%–15.5% MgO and liquidus temperatures (anhydrous, 1 atm) of 1350–1380 °C. The value of Mg # = 91.5 for phenocrystal olivine is observed in MORB glasses (Green et al., 2001) and is probably appropriate for magmas formed at relatively high degrees of melting.

We have compared the information on partial melting of lherzolite compositions at pressures to 3.5 GPa with compositions of MgO-rich glasses. We find evidence that MORB sources have slightly higher Ca/Al than MORB pyrolite (CaO/Al_2O_3 = 0.77) but not as high as Hawaiian pyrolite (0.87), MM3 lherzolite (0.90), or Tinaquillo lherzolite (0.93). Projections from olivine into the basalt tetrahedron indicate degrees of melting of spinel lherzolite along spinel lherzolite residue trends up to spinel harzburgite residue but at different pressures (depths) of magma separation from residue. Most MgO-rich MOR glasses indicate pressures of magma segregation around 1.8–2 GPa but some are as low as 1 GPa. The inference from the experimental versus natural melt comparisons that the melt fraction in partial melting of lherzolite extends to clinopyroxene-out is consistent with the same conclusion from studies of natural ocean floor peridotites (Dick and Fisher, 1984). The Baffin Island picrites (N-MORB trace element geochemistry) are at the high-temperature,

high–pressure, and high–melt fraction end of the MORB spectrum and indicate parental magmas with at least 16.7% MgO and liquidus temperatures of 1385 °C. Consistent with this inference, their liquidus spinel at Cr # = 45–57 is at the refractory end of the MORB array.

As more information is obtained on MgO-rich glasses and their spinel and olivine phenocryst compositions, it is possible that systematic patterns will be observed; for example, we would expect to be able to demonstrate increasing Cr # in spinel and increasing Mg # in olivine for liquids related by different degrees of melting (spinel lherzolite to spinel harzburgite residues) at 1.5–2 GPa. Similarly, careful examination of glasses with 7.5%–9.5% MgO may reveal populations of melts in equilibrium with plagioclase lherzolite residues (i.e., ~1 GPa, 1260 °C) and thus matching the experimental compositions and plotting appropriately in the basalt tetrahedron (cf. Falloon et al., 1999, 2001; Presnall et al., 2002). However, these will extend the spectrum of primitive MORB to lower pressures and temperatures of magma segregation, i.e., conditions that lie within the *P-T* envelope of adiabatic upwelling defined by the more magnesian glasses selected for examination in this paper.

We have argued for the existence of picritic liquids with 14%–16% MgO showing LILE and LREE depletion and with major-element compositions consistent with lherzolite to harzburgite residue at ~2 GPa (and inconsistent with plagioclase or spinel lherzolite residues at 1 GPa). These liquids require mantle potential temperatures beneath mid-ocean ridges of up to T_p~ 1430 °C.

PLATE TECTONICS WITHOUT THE "PLUME HYPOTHESIS"

Our analysis of the compositions and liquidus temperatures of parental magmas at a hotspot (Hawaii) and at mid-ocean ridge locations finds that picritic magmas with >13% MgO are characteristic of both settings and liquidus temperatures have the same range, up to 1380–1390 °C if volatile-free, but up to 1335 °C (Hawaii) and ~1355 °C (mid-ocean ridges) if volatiles (C-H-O) are included. These are the maximum temperatures, and they are not significantly different between settings. In both settings magmas may segregate at pressures and temperatures within rather than at the maximum of the adiabatic upwelling path. In seeking evidence for or against a key tenet of the "deep mantle plume" hypothesis, i.e., that an upwelling plume ("hotspot" source) had a potential temperature difference ΔT_p~ 200–250 °C above ambient mantle (MORB source), we are concerned with the maximum temperatures of typical magmas. We find that mantle potential temperatures at mid-ocean ridges are up to ~1430 °C and those beneath Hawaiian volcanos are up to ~1400 °C. As previously argued (Green et al., 1987; Green and Falloon, 1988; Green et al., 2001), the principal differences between hotspot and MOR primitive magmas and their source conditions are compositional and not thermal. The compositional differences are as follows:

Do you mean Falloon and Green, 1988, added during cleanup, or Green and Falloon, 1998?

1. Higher–(C-H-O) volatiles in hotspot source or petrogenetic process.
2. More refractory residue in hotspot petrogenesis as indicated by higher Cr # (60–75) in spinel and by harzburgite rather than lherzolite to harzburgite residues.
3. Greater heterogeneity in hotspot source as shown by variable Ca/Al, Ti/Al, Fe/Mg, and Ti/Na and by variability in isotopic and incompatible trace-element ratios.
4. Hot spot source characterized by enrichment in incompatible elements (LILE and LREE) prior to the melting and magma segregation event. There is evidence for at least two different processes of enrichment—addition of incipient melt from garnet lherzolite + (C-H-O) melting and addition of silicic melt (dacite-rhyodacite) from high-pressure melting of oceanic crust (eclogite or garnet pyroxenite melting).
5. MORB with both depletion (N-MORB, D-MORB) and enrichment (E-MORB) in incompatible elements, which is suggestive of migration of incipient melt in the garnet lherzolite + (C-H-O) system at depths >100 km.

Intraplate magmas provide strong evidence for the importance of (C-H-O) volatiles in controlling mantle melting relationships and for the extraction of magmas from the incipient melting regime, with or without lithospheric thinning and asthenospheric upwelling. They do not constrain mantle T_p but do provide a strong argument that the trace-element and isotopic signatures sometimes presented as characteristic of "mantle plume" sources (in contradistinction to MORB sources) are worldwide, present in both continental and oceanic intraplate settings and in the initial stages of plate rifting. There appears to be a seamless transition from parental intraplate magmas to magmas seen in early and waning stages of hotspot magmatism (olivine basanites, alkali olivine basalts, olivine tholeiites).

The kinematics of modern plate movements demonstrate that the causes of hotspot volcanism lie within the asthenospheric mantle and do not move with lithospheric plates. In the absence of evidence for a thermal anomaly with respect to normal mantle upwelling and magmatism at mid-ocean ridges, alternative models must be considered. Presnall and Helsey (1982) presented a model suggesting diapirism of previously subducted depleted peridotite as an appropriate cause of buoyant upwelling and hotspot magmatism without thermal anomaly. This is supported in later papers (Green et al., 1987; Green and Falloon, 1998; Green et al., 2001), in which the inferred density and compositional anomalies have additional aspects including the redox contrast between oxidized, subducted crust and lithosphere and ambient ("MORB pyrolite") mantle. Such redox fronts provide a locus of increased H_2O activity and thus of melting in the peridotite–(C-H-O) system. As Presnall and Helsey (1982) suggested, plumes or diapirs may be sourced within the upper mantle (but beneath the lithospheric plate and any dragged asthenosphere) and derived from mixtures of old subducted lithosphere and asthenospheric mantle.

It has been suggested that the characteristics of Hawaiian

"hotspot" volcanism are consistent with the initiation of diapirs or plumes within the asthenosphere at the interfaces between ambient mantle (N-MORB mantle) and old subducted crust and lithosphere (see Green, et al., 1987; Green and Falloon, 1998; Green et al., 2001). The temperature of the old subducted slab approaches that of the ambient mantle, particularly at the margins of the slab. The redox contrast between oxidized slab (fO_2 ~ IW + 3–4 log units) and asthenospheric mantle fO_2 ~ IW + 1–2 log units) means that melting will occur in the interface region as fO_2 approaches IW + 2–3 log units, i.e., peridotite + C + H_2O. The broad topographic highs on the Pacific plates, such as the Hawaiian swell, are attributed to underlying suspended or buoyant subducted slabs or delaminated lithosphere of more refractory composition and lower density than normal mantle. Hotspot volcanism is attributed to the interaction of the moving lithospheric plate over such buoyant slabs or topographic highs within or at the base of the asthenosphere rather than to the interaction of a moving lithospheric plate with an upwelling thermal plume of ΔT_p~ 200–250 °C. Our reinterpretation of hotspot volcanism, discarding the concept of deep-seated, anomalously hot mantle plumes, suggests that relative movements between hotspot sources provides a tool to investigate broad-scale flows in the asthenosphere in response to penetration of subduction of slabs into or through the transition zone. The geochemical signatures in hotspot magmas that indicate recycling of components from old subducted crust are consistent with a shallow, asthenospheric source for these recycled mantle materials and do not require the mantle plume hypothesis or return from reheating at core-mantle boundary depths.

We believe that intraplate and hotspot volcanism occur as intrinsic aspects of plate tectonics due to the subtleties of the controls of melting in the peridotite–(C-H-O) and to the stresses within, and responses of, lithospheric plates to motions over inhomogeneous mantle, with the inhomogeneity a direct consequence of plate tectonics. "Mantle plumes" may exist as thermal anomalies within the lower lithosphere and upper asthenosphere reflecting the depth of the postulated plume or hotspot source (old subducted slab), but we believe that there is strong evidence against such thermal anomalies' extending to deep levels (e.g., the core-mantle boundary) and having large ΔT_p~ 200–250 °C between plume and ambient mantle.

In our view, the melting and primary differentiation of the Earth's mantle observed at divergent plate boundaries and in intraplate settings, including hotspots, is a consequence of the plate tectonic cycle's acting on the modern Earth with mantle potential temperature T_p ~1430 °C. Plate tectonics is driven by surface cooling and lithosphere subduction (Anderson, 2000, 2001), and the argument for an additional, independent convective process represented by deep mantle thermal plumes is not supported by comparison of the magmatic products from hotspot (postulated plume), intraplate, and plate margin volcanism. Plate tectonics introduces chemical heterogeneity into the Earth's upper mantle, and chemical heterogeneity, coupled with a *P-T* envelope within a potential temperature of T_p~ 1430 °C and a global degassing of C-H-O fluids (as reduced CH_4 + H_2O at deeper levels), is responsible for the diverse magmatism observed and attributed to upper-mantle processes.

REFERENCES CITED

Anderson, D.L., 2000, Thermal state of the upper mantle: No role for mantle plumes: Geophysical Research Letters, v. 27, p. 3623–3626, doi: 10.1029/2000GL011533.

Anderson, D.L., 2001, Top-down tectonics?: Science, v. 293, p. 2016–2018, doi: 10.1126/science.1065448.

Arai, S., 1987, An estimation of the least depleted spinel on the basis of the olivine-spinel mantle array: Neues Jahrbuch für Mineralogie Monatshefte, v. 8, p. 347–354.

Bai, G., and Kohlstedt, D.L., 1992, Substantial hydrogen solubility in olivine and implications for water storage in the mantle: Nature, v. 357, p. 672–674, doi: 10.1038/357672a0.

Baker, M.B, Alves, S., and Stolper, E.M., 1996, Petrography and petrology of the HSDP lavas: Inferences from olivine phenocryst abundances and compositions: Journal of Geophysical Research, v. 101, p. 11,715–11,727.

Ballhaus, C., Berry, R.F., and Green, D.H., 1990, Oxygen fugacity controls in the Earth's upper mantle: Nature, v. 348, p. 437–440, doi: 10.1038/348437a0.

Bell, D.R., and Rossman, G.R., 1992, Water in Earth's mantle: The role of nominally anhydrous minerals: Science, v. 255, p. 1391–1397.

Berry, A.J., Hermann, J., and O'Neill, St.C.H., 2004, The water site in mantle olivine, Geochimica et Cosmochimica Acta, v. 68, no. 11, supplement 1 (Goldschmidt Conference Abstracts), p. A36.

Braun, M.G., Hirth, G., and Parmentier, E.M., 2000, The effects of deep, damp melting on mantle flow and melt generation beneath mid-ocean ridges: Earth and Planetary Science letters, v. 176, p. 339–356.

Brey, G., and Green, D.H., 1975, The role of CO_2 in the genesis of olivine melilitite: Contributions to Mineralogy and Petrology, v. 49, p. 93–103, doi: 10.1007/BF00373853.

Brey, G., and Green, D.H., 1976, Solubility of CO_2 in olivine melilitite at high pressure and role of CO_2 in the Earth's upper mantle: Contributions to Mineralogy and Petrology, v. 55, p. 217–230, doi: 10.1007/BF00372228.

Brey, G., and Green, D.H., 1977, Systematic study of liquidus phase relations in olivine melilitite + H_2O + CO_2 at high pressures and petrogenesis of an olivine melilitite magma: Contributions to Mineralogy and Petrology, v. 61, p. 141–162, doi: 10.1007/BF00374364.

Bultitude, R.J., and Green, D.H., 1968, Experimental study at high pressures on the origin of olivine nephelinite and olivine melilite nephelinite magmas: Earth and Planetary Science Letters, v. 3, p. 325–337, doi: 10.1016/0012-821X(67)90055-6.

Carey, S.W., 1958, A tectonic approach to continental drift, *in* Carey, S.W., ed., Continental drift: A symposium: Hobart, University of Tasmania, Publication 2, p. 177–355.

Clague, D.A., Weber, W.S., and Dixon, E.J., 1991, Picritic glasses from Hawaii: Nature, v. 353, p. 420–423, doi: 10.1038/353553a0.

Clarke, D.B., 1970, Tertiary basalts of Baffin Bay: Possible primary magmas from the mantle: Contributions to Mineralogy and Petrology, v. 25, p. 203–223, doi: 10.1007/BF00371131.

Dalton, J.A., and Presnall, D.C., 1998, Carbonatitic melts along the solidus of model lherzolite in the system CaO-MgO-Al_2O_3-SiO_2-CO_2 from 3 to 7 GPa: Contributions to Mineralogy and Petrology, v. 131, p. 123–135.

Danushevsky, L.V., 2001, The effect of small amounts of H_2O in crystallization of mid-ocean ridge and back arc basin magmas: Journal of Volcanology and Geothermal Research, v. 110. p. 265–280.

Danushevsky, L.V., Eggins, S.M., Falloon, T.J., and Christie, D.M., 2000, H_2O-abundance in depleted to moderately enriched mid-ocean ridge magmas, Part I: Incompatible behaviour, implications for mantle storage and origin of regional variations: Journal of Petrology, v. 41, p. 1329–1364, doi: 10.1093/petrology/41.8.1329.

Davies, G.F., 1998, Plates, plumes, mantle convection and mantle evolution, *in* Jackson, I.N.S., ed., The Earth's mantle: Composition, structure and evolution: Cambridge, England, Cambridge University Press, p. 228–258.

Dick, H.J.B., and Fisher, R.L., 1984, Mineralogic studies of the residues of mantle melting: Abyssal and alpine type peridotites, *in* Kornprobst, J., ed., Kimberlites II: The mantle and crust: Mantle relationships: Amsterdam, Elsevier, p. 295–308.

Duncan, R.A., and Green, D.H., 1987, The genesis of refractory melts in the formation of oceanic crust: Geology, v. 96, p. 326–342.

Edgar, A.D., Green, D.H., and Hibberson, W., 1976, Experimental petrology of a highly potassic magma: Journal of Petrology, v. 17, p. 339–356.

Eggins, S.M., 1992a, Petrogenesis of Hawaiian tholeiites, 1: Phase equilibria constraints: Contributions to Mineralogy and Petrology, v. 110, p. 387–397, doi: 10.1007/BF00310752.

Eggins, S.M., 1992b, Petrogenesis of Hawaiian tholeiites, 2: Aspects of dynamic melt segregation: Contributions to Mineralogy and Petrology, v. 110, p. 398–410, doi: 10.1007/BF00310753.

Elthon, D., and Scarfe, C.M., 1984, High-pressure phase equilibria of a high-magnesia basalt and the genesis of primary oceanic basalts: American Mineralogist, v. 69, p. 1–15.

Engel, A.E.J., Engel, C.G., and Havens, R.G., 1965, Chemical characteristics of oceanic basalts and the upper mantle: Geological Society of America Bulletin, v. 76, p. 719–734.

Falloon, T.J., and Green, D.H., 1988, Anhydrous melting of peridotite from 8 to 35 kb and the petrogenesis of MORB: Journal of Petrology, Special Lithosphere Issue, p. 379–414.

Falloon, T.J., and Green, D.H., 1989, The solidus of carbonated, fertile peridotite: Earth and Planetary Science Letters, v. 94, p. 364–370, doi: 10.1016/0012-821X(89)90153-2.

Falloon, T.J., and Green, D.H., 1990, Solidus of carbonated fertile peridotite under fluid-saturated conditions: Geology, v. 18, p. 195–199, doi: 10.1130/0091-7613(1990)0182.3.CO;2.

Falloon, T.J., Green, D.H., Hatton, C.J., and Harris, K.L., 1988, Anhydrous partial melting of fertile and depleted peridotite from 2 to 30 kbar and application to basalt petrogenesis: Journal of Petrology, v. 29, p. 257–282.

Falloon, T.J., Green, D.H., Danyushevsky, L.V., and Faul, U.H., 1999, Peridotite melting at 1.0 and 1.5 GPa: An experimental evaluation of techniques using diamond aggregates and mineral mixes for determination of near-solidus melts: Journal of Petrology, v. 40, p. 1343–1375, doi: 10.1093/petrology/40.9.1343.

Falloon, T.J., Danushevsky, L.V., and Green, D.H., 2001, Reversal experiments on partial melt compositions produced by peridotite–basalt sandwich experiments: Journal of Petrology, v. 42, p. 2363–2390, doi: 10.1093/petrology/42.12.2363.

Faul, U., 2001, Melt retention and segregation at mid-ocean ridges: Earth and Planetary Science Letters, v. 176, p. 339–356.

Foley, S.F., 1989, Experimental constraints on phlogopite chemistry in lamproites, 1: The effect of water activity and oxygen fugacity: European Journal of Mineralogy, v. 1, p. 411–426.

Ford et al. _____ **[AQ2]**.

You intended to add this, but didn't. Please add it now.

Francis, D., 1985, The Baffin Bay picrites and the value of picrites as analogues of primary magmas: Contributions to Mineralogy and Petrology, v. 89, p. 144–145, doi: 10.1007/BF00379449.

Frey, F.A., Green, D.H., and Roy, S.D., 1978, Integrated models of basalt petrogenesis: A study of quartz tholeiites to olivine melilitites from southeastern Australia utilizing geochemical and experimental petrological data: Journal of Petrology, v. 19, p. 463–513.

Garcia, M.O., Muenow, D.W., Aggrey, K.E., and O'Neil, J.R., 1989, Major element, volatile and stable isotope geochemistry of Hawaiian submarine tholeiitic glasses: Journal of Geophysical Research, v. 94, p.10,525–10,538.

Green, D.H., 1970, A review of experimental evidence on the origin of basaltic and nephelinitic magmas: Physics of the Earth and Planetary Interiors, v. 3, p. 221–235, doi: 10.1016/0031-9201(70)90060-9.

Green, D.H., 1971, Compositions of basaltic magmas as indicators of conditions of origin: Application to oceanic volcanism, Philosophical Transactions of the Royal Society, London (Ser. A), v. 268, p. 707–725.

Green, D.H., 1973a, Conditions of melting of basanite magma from garnet peridotite: Earth and Planetary Science Letters, v. 17, p. 456–465, doi: 10.1016/0012-821X(73)90214-8.

Green, D.H., 1973b, Experimental melting studies on a model upper mantle composition at high pressure under water-saturated and water-undersaturated conditions: Earth and Planetary Science Letters, v. 19, p. 37–53, doi: 10.1016/0012-821X(73)90176-3.

Green, D.H., and Falloon, T.J., 1998, Pyrolite: A Ringwood concept and its current expression, *in* Jackson, I.N.S., ed., The Earth's mantle: Composition, structure, and evolution: Cambridge, England, Cambridge University Press, p. 311–380.

Green, D.H., and Hibberson, W., 1970, Experimental duplication of conditions and precipitation of high pressure phenocrysts in a basaltic magma: Physics of the Earth and Planetary Interiors, v. 3, p. 247–254, doi: 10.1016/0031-9201(70)90063-4.

Green, D.H., Hibberson, W.O., and Jaques, A.L., 1979, Petrogenesis of mid-ocean ridge basalts, *in* McElhinny, M.W., ed., The Earth: Its origin, structure and evolution: London, Academic Press, p. 265–290.

Green, D.H., and Liebermann, R.C., 1976, Phase equilibria and elastic properties of a pyrolite model for the oceanic upper mantle: Tectonophysics, v. 32, p. 61–92, doi: 10.1016/0040-1951(76)90086-X.

Green, D.H., and Ringwood, A.E., 1967a, An experimental investigation of the gabbro to eclogite transformation and its petrological applications: Geochimica et Cosmochimica Acta, v. 31, p. 767–833.

Green, D.H., and Ringwood, A.E., 1967b, The genesis of basaltic magmas: Contributions to Mineralogy and Petrology, v. 15, p. 103–190, doi: 10.1007/BF00372052.

Green, D.H., and Wallace, M.E., 1988, Mantle metasomatism by ephemeral carbonatite melts: Nature, v. 336, p. 459–462.

Green, D.H., Edgar, A.D., Beasley, P.H., Kiss, E., and Ware, N.G., 1974, Upper mantle source for some hawaiites, mugearites and benmoreites: Contributions to Mineralogy and Petrology, v. 48, p. 33–43, doi: 10.1007/BF00399108.

Green, D.H., Falloon, T.J., and Taylor, W.R., 1987, Mantle-derived magmas: Roles of variable source peridotite and variable C-H-O fluid compositions, *in* Mysen, B.O., ed., Magmatic processes: Physicochemical principles: University Park, Pennsylvania, Geochemcal Society, Special Publication 1, p. 139–154.

Green, D.H., Falloon, T.J., Eggins, S.M., and Yaxley, G.M., 2001, Primary magmas and mantle temperatures: European Journal of Mineralogy, v. 13, p. 437–451, doi: 10.1127/0935-1221/2001/0013-0437.

Green, D.H., Schmidt, M.W., and Hibberson, W., 2004, Ultra-calcic magmas generated from Ca-depleted mantle: An experimental study on the origin of ankaramites: Journal of Petrology, v. 45, p. 391–403, doi: 10.1093/petrology/egg101.

Hauri, E.H., Gaetani, G.A., and Green, T.H., 2004, Partitioning of H_2O between mantle minerals and silicate melts: Geochimica et Cosmochimica Acta, v. 68, no. 11, supplement 1 (Goldschmidt Conference Abstracts), p. A33.

Hirschmann, M., 2000, Mantle solidus: Experimental constraints and the effects of peridotite composition. Geochemistry, Geophysics, Geosystems, v. 1, no. 10, doi: 10.1029.2000GG000070.

Ingrin, J., and Skogby, H., 2000, Hydrogen in nominally anhydrous upper-mantle minerals: Concentration levels and implications: European Journal of Mineralogy, v. 12, p. 543–570.

Jaques, A.L., and Green, D.H., 1980, Anhydrous melting of peridotite at 0–15 kb pressure and the genesis of tholeiitic basalts: Contributions to Mineralogy and Petrology, v. 73, p. 287–310, doi: 10.1007/BF00381447.

Kamenetsky, V.S., Eggins, S.M., Crawford, A.J., Green, D.H., Gasparon, M., and Falloon, T.J., 1998, Calcic melt inclusions in primitive olivine at 32°N MAR: Evidence for melt-rock reaction/melting involving clinopyroxene-rich lithologies during MORB generation: Earth and Planetary Science Letters, v. 160, p. 115–132, doi: 10.1016/S0012-821X(98)00090-9.

Kelemen, P.B., Dick, H.J.B., and Quick, J.E., 1992, Formation of harzburgite by

pervasive melt/rock reaction in the upper mantle: Nature, v. 358, p. 635–641, doi: 10.1038/358635a0.

Keppler, H., Wiedenbeck, M., and Shcheka, S.S., 2003, Carbon solubility in olivine and the mode of carbon storage in the Earth's mantle: Nature, v. 424, p. 414–416, doi: 10.1038/nature01828.

Klein, E.M., and Langmuir, C.H., 1987, Global correlations of ocean ridge basalt chemistry with axial depth and crustal thickness: Journal of Geophysical Research, v. 92, p. 8089.

Kurosawa, M., Yurimoto, H., and Sueno, S., 1997, Patterns in the hydrogen and trace element compositions of mantle olivines: Physics and Chemistry of Minerals, v. 24, p. 385–395, doi: 10.1007/s002690050052.

McKenzie, D., and Bickle, M.J., 1988, The volume and composition of melt generated by extension of the lithosphere: Journal of Petrology, v. 29, p. 625–679.

Mengel, K., and Green, D.H., 1989, Stability of amphibole and phlogopite in metasomatized peridotite under water-saturated and water-undersaturated conditions: Fourth International Kimberlite Conference, Perth, Western Australia: Kimberlites and Related Rocks: Their Composition, Occurrence, Origin and Emplacement: Geological Society of Australia, Special Publication 14: Carlton, Australia, Blackwell Scientific Publications, p. 571–581.

Michael, P.J., 1988, The concentration, behaviour and storage of H_2O in the suboceanic upper mantle: Implications for mantle metasomatism: Geochimica et Cosmochimica Acta, v. 52, p. 555–566.

Minarik, W.G., and Watson, E.B., 1995, Interconnectivity of carbonate melt at low melt fraction: Earth and Planetary Science Letters, v. 133, p. 423 –437.

Morgan, W.J., 1971, Convection plumes in the lower mantle: Nature, v. 230, p. 42–43.

Niida, K., and Green, D.H., 1999, Stability and chemical composition of pargasitic amphibole in MORB pyrolite under upper mantle conditions: Contributions to Mineralogy and Petrology, v. 135, p. 18–40, doi: 10.1007/s004100050495.

Norman, M.D., and Garcia, M., 1999, Primitive magmas and source characteristics of the Hawaiian plume: Petrology and geochemistry of shield picrites: Earth and Planetary Science Letters, v. 168, p. 27–44, doi: 10.1016/S0012-821X(99)00043-6.

Norman, M.D., Garcia, M., Kamenetsky, V.S., and Nielson, R.L., 2002, Olivine-hosted melt inclusions in Hawaiian picrites: Equilbration, melting and plume source characteristics: Chemical Geology, v. 183, p. 143–168, doi: 10.1016/S0009-2541(01)00376-X.

Odling, N.W.A., 1989, The role of sulphur in upper mantle processes [Ph.D. thesis]: Hobart, University of Tasmania.

O'Hara, M.J., 1968, Are any ocean floor basalts primary magma?: Nature, v. 220, p. 683–686.

O'Reilly, S.Y., and Griffin, W.L., 1988, Mantle metasomatism beneath Western Victoria: Metasomatic processes in Cr-diopside lherzolites: Geochemica et Cosmochimica Acta, v. 52, p. 433–447, doi: 10.1016/0016-7037(88)90099-3.

Presnall, D.C., and Helsey, C.E., 1982, Diapirism of depleted peridotite: A model for the origin of hot spots: Physics of the Earth and Planetary Interiors, v. 29, p. 148–160, doi: 10.1016/0031-9201(82)90069-3.

Presnall, D.C., Gudfinnsson, G.H., and Walker, M.J., 2002, Generation of mid ocean ridge basalts at pressures from 1 to 7 GPa: Geochimica et Cosmochimica Acta, v. 66, p. 2073–2090, doi: 10.1016/S0016-7037(02)00890-6.

Price, R.C., and Green, D.H., 1972, Lherzolite nodules in a "mafic phonolite" from North East Otago, New Zealand: Nature, v. 235, p. 133–134.

Rhodes, J.M., 1996, Geochemical stratigraphy of lava flows sampled by the Hawaiian Scientific Drilling Project: Journal of Geophysical Research, v. 101, p. 11,729–11,746, doi: 10.1029/95JB03704.

Robillard, I., Francis, D., and Ludden, J.N., 1992, The relationship between E- & N-type magmas in the Baffin Bay lavas: Contributions to Mineralogy and Petrology, v. 112, p. 230–241, doi: 10.1007/BF00310457.

Ryabchikov, I.E., and Green, D.H., 1978, The role of carbon dioxide in the petrogenesis of highly potassic magmas: Problems of the petrology of the Earth's crust and upper mantle: Trudi, Akademiya Nauk USSR, Siberian Region, Institute for Geology and and Geophysics, p. 49–64.

Saal, A.E., Hauri, E.H., Langmuir, C.H., and Perfit, M.R., 2002, Vapour undersaturation in primitive mid-ocean-ridge basalt and the volatile content of Earth's upper mantle: Nature, v. 419, p. 451–455, doi: 10.1038/nature01073..

Schulze, D.J., Harte, B., Valley, J.W., Brenan, J.M., and Channer, D.M.R., 2003, Extreme crustal oxygen isotope signatures preserved in coesite in diamond: Nature, v. 423, p. 68, doi: 10.1038/nature01615.

Seaman, C., Sherman, S., Garcia, M., Baker, M., and Stolper, E. M., 2004, Volatiles in glasses from the HSDP2 drill core, Geochemistry, Geophysics, Geosystems, v. 5, Q09G16, doi: 10.1029/2003GC000596.

Stolper, E.M., 1980, A phase diagram for mid-ocean ridge basalts: Preliminary results and implications for petrogenesis: Contributions to Mineralogy and Petrology, v. 74, p. 13–27, doi: 10.1007/BF00375485.

Stolper, E.M., Sherman, S., Garcia, M., Baker, M., and Seaman, C., 2004, Glass in the submarine section of the HSDP2 drill core: Hilo, Hawaii: Geochemistry, Geophysics, Geosystems, v. 5, Q07G15, doi: 10.1029/2003GC000553.

Sun, S.-S., and McDonough, W.F., 1989, Chemical and isotopic systematics of oceanic basalts: Implications for mantle compositions and processes, *in* Saunders, A.D., and Norry, M.J., eds., Magmatism in the ocean basins: Geological Society of London, Special Publication 42, p. 313–345.

Sweeney, R.J., Falloon, T.J., and Green, D.H., 1995, Experimental constraints on the possible mantle origin of natrocarbonatite, *in* Bell, K., and Keller, J., eds., Carbonatite volcanism: Oldoinyo Lengai and the petrogenesis of natrocarbonatites: Berlin, Springer-Verlag, p. 190–207.

Taylor, W.R., and Green, D.H., 1988, Measurement of reduced peridotite-C-O-H solidus and implications for redox melting of the mantle: Nature, v. 332, p. 349–352.

Wagner, T.P., and Grove, T.L., 1998, Melt/harzburgite reaction in the petrogenesis of tholeiitic magma from Kilauea Volcano, Hawaii: Contributions to Mineralogy and Petrology, v. 131, p. 1–12, doi: 10.1007/s004100050374.

Wallace, M.E., and Green, D.H., 1988, An experimental determination of primary carbonatite magma composition: Nature, v. 335, p. 343–346, doi: 10.1038/335343a0.

Wallace, M.E., and Green, D.H., 1991, The effect of bulk rock compositions on the stability of amphibole in the upper mantle: Implications for solidus positions and mantle metasomatism: Mineralogy and Petrology, v. 44, p. 1–19.

Wilson, J.T., 1963, Hypothesis of Earth's behaviour: Nature, v. 198, p. 925–929.

Worner, G., and Zipfel, J., 1996, A mantle P-T path for the Rose Sea Rift Margin, Antarctica, derived from mineral zoning in peridotite xenoliths: Geologisches Jahrbuch, v. B89, p. 157–167.

Wyllie, P.J., 1987, Discussion of recent papers on carbonated peridotite, bearing on mantle metasomatism and magmatism: Earth and Planetary Science Letters, v. 82, p. 391–397, doi: 10.1016/0012-821X(87)90213-5.

Yaxley, G.M., and Green, D.H., 1996, Experimental reconstruction of sodic dolomitic carbonatite melts from metasomatised lithosphere: Contributions to Mineralogy and Petrology, v. 124, p. 359–369, doi: 10.1007/s004100050196.

Yaxley, G.M., and Green, D.H., 1998, Reactions between eclogite and peridotite: Mantle refertilization by subduction of oceanic crust: Schweizerische Mineralogische und Petrographische Mitteilungen, v. 78, p. 243–255.

Yaxley, G.M., Crawford, A.J., and Green, D.H., 1991, Evidence for carbonatite metasomatism in spinel peridotite xenoliths from W. Victoria, Australia: Earth and Planetary Science Letters, v. 107, p. 305–317, doi: 10.1016/0012-821X(91)90078-V.

Yaxley, G.M., Green, D.H., and Kamenetsky, V., 1998, Carbonatite metasomatism in the southeastern Australian lithosphere: Journal of Petrology, v. 39, p. 1917–1930, doi: 10.1093/petrology/39.11.1917.

Yaxley, G.M., Kamenetsky, V.S., Kamenetsky, M., Norman, M.D., and Francis, D., 2004, Origins of compositional heterogeneity in olivine-hosted melt inclusions from the Baffin Id Picrites: Contributions to Mineralogy and Petrology, v. 148, p. 426–442, doi: 10.1007/S00410-004-0613-Z.

Yoder, H.S., and Tilley, C.E., 1962, Origin of basalt magmas, an experimental study of natural and synthetic rock systems: Journal of Petrology, v. 3, p. 342–532.

Manuscript Accepted by the Society January 3, 2005

Printed in the USA

Page 248 is blank